Aqueous-phase reforming of renewables for selective hydrogen production in the presence of supported platinum catalysts

Alexey V. Kirilin

Laboratory of Industrial Chemistry and Reaction Engineering
Process Chemistry Centre
Department of Chemical Engineering
Åbo Akademi University
Turku/Åbo 2013

Aqueous-phase reforming of renewables for selective hydrogen production in the presence of supported platinum catalysts

Alexey V. Kirilin

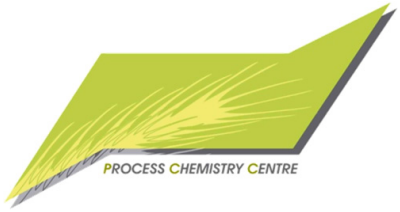

Laboratory of Industrial Chemistry and Reaction Engineering
Process Chemistry Centre
Department of Chemical Engineering
Åbo Akademi University
Turku/Åbo, Finland 2013

Supervised by

Professor Dmitry Yu. Murzin
Åbo Akademi University, Finland

Academy Professor Tapio Salmi
Åbo Akademi University, Finland

Professor J.-P.Mikkola
Åbo Akademi University, Finland & Umeå University, Sweden

Co-supervised by

Professor Leonid M. Kustov
N.D. Zelinsky Institute of Organic Chemistry RAS, Russia

Reviewers

Dr. Juan Carlos Serrano Ruiz
Abengoa Research, Spain

Dr. Irina Simakova
Boreskov Institute of Catalysis, Russia

Opponent

Dr. Juan Carlos Serrano Ruiz
Abengoa Research, Spain

ISBN 978-952-12-2974-9
Painosalama Oy – Turku, Finland 2013

Посвящается семье

Preface

This work was performed between 2009 and 2013 at the Laboratory of Industrial Chemistry and Reaction Engineering, Department of Chemical Engineering at Åbo Akademi University. Research is a part of activities at the Åbo Akademi Process Chemistry Centre (PCC), a centre of excellence financed by Åbo Akademi University.

I would like to thank the squad of professors supervising and advising me during my PhD studies at Åbo Akademi: Professors Dmitry Murzin, Jyri-Pekka Mikkola, Tapio Salmi, Johan Wärnå and Leonid Kustov.

Professor Dmitry Murzin is acknowledged for all his brilliant knowledge and valuable experience that he shared with me during these years. Deep scientific discussions are gratefully acknowledged. The contribution to my fledging as a scientist is sincerely appreciated. Professor Jyri-Pekka Mikkola is acknowledged for all what he has done for me and keeps on doing within science and much beyond. I would like to thank Professor Tapio Salmi for his expertise and support in many aspects having impact on research and general life in Finland. Additionally, I appreciate great opportunity to work at the brilliant Laboratory and conduct research in the fascinating area of catalysis for biomass conversion. I would like to thank Professor Johan Wärnå for sharing his experience in kinetic modeling. Professor Leonid Kustov is gratefully acknowledged for his valuable advice, supervision and general support.

I would like to thank all the co-authors and co-workers from Åbo Akademi University (Finland), Zelinsky Institute of Organic Chemistry (Russia), Umeå University (Sweden), Queen's University of Belfast (UK), University Erlangen-Nuremberg (Germany), University of Oulu (Finland) for fruitful and successful collaboration. I hope that our cooperation will continue in future.

Herein I am happy to acknowledge my friends in Finland and abroad. I would like to thank them for their constant support and encouragement, for never letting me down during hard times. Pasi Tolvanen, Anton Tokarev, Pavel and Alexey Grigoriev, Bartosz Rozmysłowicz, Olga Simakova, Gerson Martin, Viktor Vorobyev, all my friends at Åbo Akademi and researchers from Laboratory of Industrial Chemistry and Reaction Engineering are gratefully acknowledged. I thank Docent Päivi Mäki-Arvela and Dr. Kari Eränen for their assistance.

Last, but not least, I would like to express my deepest respect to my family, which lives in Moscow, and has been always supporting me in everything and every case. Especially, I would like to say thank you to my parents Nadezhda and Viktor (1953-2007) for encouraging me to do exact sciences. My father was always pushing me to study mathematics and physics hoping that I would follow his track, but I have chosen chemistry. On top of that, I express my appreciation to my girlfriend Julia for her love and endless patience.

The Academy of Finland in collaboration with the North European Innovative Energy Research Programme (N-Inner, 2010-2013), the Graduate School in Chemical Engineering (GSCE, 2010-2013), Fortum Foundation (2009-2011) and Haldor Topsøe Scholarship Program (2010-2012) are gratefully acknowledged for financial support. In addition, the COST–Action CM0903 (UbioChem, 2010-2013) is acknowledged.

Alexey Kirilin
November 2013, Turku, Finland

Abstract

Alexey V. Kirilin

Keywords: platinum, aqueous reforming, sorbitol, xylitol, kinetics, reaction mechanism

Aqueous-phase reforming of renewables for selective hydrogen production in the presence of supported Pt catalysts

The evolution of our society is impossible without a constant progress in life-important areas such as chemical engineering and technology. Innovation, creativity and technology are three main components driving the progress of chemistry further towards a sustainable society. Biomass, being an attractive renewable feedstock for production of fine chemicals, energy-rich materials and even transportation fuels, captures progressively new positions in the area of chemical technology. Knowledge of heterogeneous catalysis and chemical technology applied to transformation of biomass-derived substances will open doors for a sustainable economy and facilitates the discovery of novel environmentally-benign processes which probably will replace existing technologies in the era of biorefinary.

Aqueous-phase reforming (APR) is regarded as a promising technology for production of hydrogen and liquids fuels from biomass-derived substances such as C_3-C_6 polyols. In the present work, aqueous-phase reforming of glycerol, xylitol and sorbitol was investigated in the presence of supported Pt catalysts. The catalysts were deposited on different support materials, including Al_2O_3, TiO_2 and carbons. Catalytic measurements were performed in a laboratory-scale continuous fixed-bed reactor.

An advanced analytical approach was developed in order to identify reaction products and reaction intermediates in the APR of polyols. The influence of the substrate structure on the product formation and selectivity in the APR reaction was also investigated, showing that the yields of the desired products varied depending on the substrate chain length. Additionally, the influence of bio-ethanol additive in the APR of glycerol and sorbitol was studied. A reaction network was advanced explaining the formation of products and key intermediates.

The structure sensitivity in the aqueous-phase reforming reaction was demonstrated using a series of platinum catalysts supported on carbon with different Pt cluster sizes in the continuous fixed-bed reactor. Furthermore, a correlation between texture physico-chemical properties of the catalysts and catalytic data was established.

The effect of the second metal (Re, Cu) addition to Pt catalysts was investigated in the APR of xylitol showing a superior hydrocarbon formation on PtRe bimetallic catalysts compared to monometallic Pt.

On the basis of the experimental data obtained, mathematical modeling of the reaction kinetics was performed. The developed model was proven to successfully describe experimental data on APR of sorbitol with good accuracy.

Referat

Alexey V. Kirilin

Nyckelord: platina, vattenfasreformering, sorbitol, xylitol, kinetik, reaktionsmekanism

Vattenfasreformering av förnyelsebara råvaror för selektiv väteproduktion i närvaro av platinakatalysatorer

Utveckling av vårt samhälle är omöjlig utan framsteg av de vetenskapsgsgrenar som är centrala för ett modernt människoliv. Den centrala vetenskapen i detta avseende är kemisk teknologi och kemiingenjörsvetenskap. Innovation, kreativitet och teknologi är de tre huvudkomponenter, som driver kemin framåt mot ett hållbart samhälle. Biomassa, som är en synnerligen attraktiv, förnyelsebar råvara för framställning av finkemikalier, energirika material och bränslekomponenter, erövrar ständigt nya positioner inom den kemiska teknologin. Kunskap och färdighet i heterogen katalys och kemisk teknologi öppnar dörrar för en hållbar ekonomi och möjliggör nya, miljövänliga processer, vilka eventuellt kommer att ersätta existerande teknologier i bioraffinaderiernas tidevarv.

Vattenfasreformering (APR) anses vara en mycket lovande teknologi för produktion av vätgas och vätskeformiga bränslen utgående från komponenter i biomassa, t.ex. C_3-C_6-polyoler. I detta arbete studerades vattenfasreformering av glycerol, xylitol och sorbitol i närvaro av burna platinakatalysatorer. Olika katalysatorbärarmaterial användes: aluminiumoxid, titandioxid och kolmaterial. Katalytiska experiment genomfördes i en kontinuerlig packad bäddreaktor i laboratorieskala.

En avancerad analytisk metod utvecklades för att identifiera reaktionsprodukter och intermediärer, som uppstår vid vattenfasreformering av polyoler. Inverkan av reaktantmolekylens struktur på produktbildningen varierade, beroende av reaktantmolekylens kedjelängd. Dessutom undersöktes, hur tillsats av bioetanol inverkade vattenfasreformeringen av glycerol och sorbitol. Reaktionsschemat som syntetiserades förklarar bildningen av reaktionsprodukter och -intermediärer.

Strukturkänsligheten för vattenfasreformeringsprocessen demonstrerades genom att använda flera kolburna platinakatalysatorer med olika platinaklusterstorlekar i den kontinuerliga packad bäddreaktorn. En korrelation mellan katalysatorernas strukturella fysikalisk-kemiska egenskaper och experimentella data utvecklades.

Tillsats av en annan metall (renium, koppar) på platinakatalysatorn undersöktes för vattenfasreformering av xylitol. Bildning av kolväten ökade kraftigt på bimetalliska platina-reniumkatalysatorer.

Reaktionskinetiken, d.v.s. reaktionshastigheter modellerades matematiskt på basis av experimentella katalytiska data. Modellen beskrev framgängsrikt, med en god noggrannhet vattenfasreformeringen av xylitol.

Реферат

Ключевые слова: платина, водяной риформнг, сорбитол, ксилитол, кинетика, механизм реакции

В настоящей работе был изучен водяной риформинг компонентов биомассы с целью селективного получения водорода в присутствии нанесенных платиновых катализаторов.

Развитие современного общества невозможно без постоянного прогресса в таких жизненно важных областях, как химическая технология и катализ. Инновации, изобретения и новые технологии, являющиеся ключевыми компонентами в обеспечении развития химической науки для производства препаратов тонкой химии, энергоемких веществ и топлив, занимают все большие позиции в химической технологии. Достижения в области гетерогенного катализа и химической технологии, применяемые к превращениям веществ, получаемых из биомассы, в скором будущем откроют двери для устойчивой экономики и новых экологически безопасных производств, которые однажды придут на смену существующим процессам.

Водяной риформинг (ВР) считается одним из наиболее перспективных процессов производства водорода (водород-содержащего газа) и компонентов топлив из веществ, получаемых в результате переработки биомассы, таких как, например, полиолы C_3-C_6. В настоящей работе изучался водяной риформинг глицерина, ксилитола и сорбитола в присутствии нанесенных платиновых катализаторов. Катализаторы приготовлены путем нанесения платины на различные носители, такие как оксид алюминия, титана, а также различные углеродные материалы. Каталитические испытания проводили на установке проточного типа с неподвижным слоем катализатора в интервале температур 210-225°C при давлении 29,3 атм.

В рамках работы разработан аналитический метод, позволяющий количественно определять сложный состав реакционной смеси в процессе водяного риформинга полиолов. Изучено влияние структуры субстрата на образование продуктов реакции. Установлено, что длина углеродной цепи субстрата влияет на выход целевых продуктов реакции. Кроме того, изучено влияние добавления био-этанола как второго компонента реакции ВР сорбитола и глицерина. На основании полученных данных предложена схема образования продуктов и промежуточных соединений.

В работе исследована структурная чувствительность реакции на примере серии катализаторов Pt/C. Установлена корреляция каталитической активности и физико-химических свойств катализаторов.

Установлено влияние второго металлического компонента (Re, Cu) на образование целевых продуктов реакции ВР полиолов. Показано, что биметаллический нанесенный PtRe катализатор проявляет более высокую активность в образовании углеводородов по сравнению с монометаллическим платиновым образцом.

В рамках исследования разработана кинетическая модель на основе экспериментальных данных и представлений о механизме. Предложенная модель успешно применена для описания экспериментальных данных ВР сорбитола.

List of publications

I. **A.V. Kirilin**, A.V. Tokarev, E.V. Murzina, L.M. Kustov, J.-P. Mikkola, D.Yu. Murzin, "Reaction Products and Transformations of Intermediates in the Aqueous-Phase Reforming of Sorbitol", *ChemSusChem*, **2010**, *3*, 708-718.
Contribution: performed the experiments, wrote and edited the article.

II. A.V. Tokarev, **A.V. Kirilin**, E.V. Murzina, K. Eränen, L.M. Kustov, D.Yu. Murzin, J.-P. Mikkola, "The Role of Bioethanol in Aqueous Phase Reforming to Sustainable Hydrogen", *J. Hydr. En.*, **2010**, *35*, 12642-12649.
Contribution: contributed to performing the experiments and editing the article.

III. **A.V. Kirilin**, A.V. Tokarev, L.M. Kustov, T. Salmi, J.-P. Mikkola, D.Yu. Murzin, "Aqueous-phase reforming of sugar alcohols: influence of substrate structure", *Appl.Catal. A: General,* **2012***, 435-436*, 172-180.
Contribution: performed the experiments, wrote and edited the article.

IV. **A.V. Kirilin**, A.V. Tokarev, H. Manyar, C.Hardacre, T.Salmi, J.-P. Mikkola, D. Yu. Murzin, "Aqueous-phase reforming of xylitol over Pt-Re bimetallic catalyst", *Catalysis Today*., **2013**, http://dx.doi.org/10.1016/j.cattod.2013.09.020, *in press.*
Contribution: performed the experiments, wrote and edited the article.

V. **A.V. Kirilin**, B. Hasse A.V. Tokarev, L. M. Kustov, G. N. Baeva, G. O. Bragina, A. Yu. Stakheev, A.-R. Rautio, T. Salmi, B.J.M. Etzold, J.-P. Mikkola, D. Yu. Murzin, "Aqueous-phase reforming of xylitol over Pt/C and Pt/TiC-CDC catalysts", *Catal. Sci. tech.*,, **2013**, *accepted for publication.*
Contribution: performed the experiments, wrote and edited the article.

VI. **A.V. Kirilin**, A.V. Tokarev, J. Wärnå, D. Yu. Murzin, "Aqueous-phase reforming of sorbitol: kinetic modelling", *Ind. Eng. Chem. Res.*, **2013**, *submitted.*
Contribution: performed the experiments, contributed to modeling of the results, wrote the article.

List of related publications

1. D.A. Boga, A.V. Tokarev, **A.V. Kirilin**, D.Yu. Murzin, P.C.A. Bruijnincx, J.-P. Mikkola. B.M. Weckhuysen, "Aqueous-Phase Reforming of Xylitol for the Production of Hydrogen: Influence of of Support and Process Conditions on Catalyst Activity and Selectivity", *Catal. Tod.*, **2013**, *submitted*.
2. **A.V. Kirilin,** A.V. Tokarev, D.Yu. Murzin, J.-P. Mikkola, "Catalytic conversion of biomass-derived chemicals for hydrogen and liquid fuel production", COST Action CM0903 UBIOCHEM I, Utilisation of biomass for fuels and chemicals, 13-15th May 2010, University of Cordoba, Spain, O5, p.24 (oral presentation)
3. **A. Kirilin,** A. Tokarev, T. Salmi, J.-P. Mikkola, D.Yu. Murzin, "Aqueous phase reforming of biomass derived alcohols and polyols to hydrogen and fuel components", Chemreactor-19, 5-9th September 2010, Vienna, Austria, PP-III-29, p.492 (CD) (poster presentation).
4. **A. V. Kirilin**, A. Tokarev, L. M. Kustov, T. Salmi, J.-P. Mikkola, D. Yu. Murzin, "Aqueous phase reforming of biomass feedstocks as an approach to hydrogen production", EUROPACAT X, 28th August – 2nd September 2011, Glasgow, Scotland (oral presentation).
5. **A.V. Kirilin**, A.V. Tokarev, D.Yu. Murzin, J.-P. Mikkola, "Selective hydrogen production from renewables: catalytic conversion of biomass-derived C5-C6 sugar alcohols via aqueous phase reforming", ChemPor-2011, 5-7th September 2011, Caparica, Portugal (poster presentation).
6. **A.V. Kirilin**, A.V. Tokarev, L. M. Kustov, D.Yu. Murzin, J.-P. Mikkola "Catalytic production of hydrogen via aqueous phase reforming of renewables", First international congress on catalysis for biorefinaries CatBior, 2-5th October 2011, Malaga, Spain (oral presentation).
7. **A.V. Kirilin**, A.V. Tokarev, L.M. Kustov, D.Yu. Murzin, "Production of hydrogen via aqueous phase reforming of biomass components", First Russian Congress on Catalysis, ROSCATALYSIS, 3-7th October 2011, Moscow, Russia (oral presentation).
8. **A. Kirilin**, A. Tokarev, T. Salmi, D.Yu. Murzin, J.-P. Mikkola, "Aqueous phase reforming of biomass feedstocks: an approach to sustainable hydrogen and liquid fuels", 243rd American Chemical Society National Meeting, 24–29th March 2012, San Diego, California, USA, Preprints of Symposia – American Chemical Society, Division of Fuel Chemistry, **2012**, *57*, 614 (oral presentation).
9. **A. Kirilin**, A. Tokarev, D.Yu. Murzin, J.-P. Mikkola, "Bio-hydrogen via aqueous phase reforming of sugar alcohols", International Congress on Hydrogen Production, 24–27th June 2012, Seoul, South Korea, Book of abstracts, p. 135–136 (oral presentation).
10. **A. Kirilin**, A. Tokarev, T. Salmi, J.-P. Mikkola, D.Yu. Murzin, "Aqueous phase reforming of biomass feedstocks: an approach to sustainable hydrogen and liquid fuels", 15th International Congress on Catalysis, 1–6th July 2012, Munich, Germany, abs. No. 7351 (poster presentation).

CONTENTS

1. Introduction

The evolution of our society is impossible without constant progress in the life-important areas such as chemical engineering and technology. Innovation, creativity and technology are three main components driving the progress of chemistry further towards a sustainable society.

Global energy consumption, especially in the developing countries, leads to a huge demand for fossil fuels. Uneven distribution of natural resources such as oil, gas and coal encourages scientists all over the world to search alternative ways for the production of energy-rich materials from renewable resources. Undoubtedly, biomass is one of the most attractive renewable sources available on our planet. The importance of the utilization of biomass-derived components to produce fuels, energy-rich materials and commodities is justified not only by the limited amount of fossil fuel resources, but also by a fundamental interest and unique opportunities to discover novel processes and technologies which will replace the existing ones in the future. The utilization of renewables in chemical processes is an environmentally benign and important in terms of preserving the nature for future generations. Another significant reason to perform research in the area of biomass valorization is to educate the population of the planet to avoid unnecessary wasting of energy and to consume it in a more deliberate way. Therefore, biomass and biomass-derived products in the form of ready-to-use chemicals attract nowadays much attention all over the world[1].

The main components of wood biomass are cellulose (40-50%), hemicelluloses (15-30%) and lignin (15-33%)[2]. There are several pathways of biomass transformation into valuable products and fuels, i.e. valorization of biomass. The pathways include combustion, gasification, pyrolysis and hydrolysis after delignification which is followed by transformation and/or the upgrading of components derived into hydrogen, fuels and chemicals[1]. Gasification of biomass is mainly used for the production of syn-gas (CO and H_2) which can be further used in Fischer-Tropsch synthesis, gas-to-liquids processes and water-gas shift reaction to produce alkanes, alcohols[3] and hydrogen. Bio-oils, being a mixture of oxygenates resulted from catalytic or non-catalytic pyrolysis of wood biomass can also be considered for hydrogen production[3], however, the yields of desired products are still to be improved[4]. It is important to note that gasification and production of bio-oils are extremely energy-consuming processes. Typically, the reactions result in non-selective product formation, low yields of the desired products and severe catalyst deactivation.

A much more attractive way to utilize biomass sources for production of chemicals and fuels includes aqueous-phase processing technologies. Thereby, oxygenates which are obtained from

lignocellulosic biomass can be catalytically converted to hydrogen[3], transportationary fuels[5,67] and chemicals via aqueous-phase processing[8].

Looking deeper into the chemical composition of wood biomass it can be noticed that polysaccharides, i.e. cellulose, hemicelluloses and pectins along with lignin, are the main constituents of wood[9]. Cellulose can be used for production of glucose, which can be hydrogenated to sorbitol. The high content of hemicelluloses, xylans, in hardwood species renders this source attractive for xylose and further, xylitol production[10]. In some species of hardwood, the content of xylose in the heartwood part can reach 26 wt. %, or even more (dry mass)[11]. The corresponding sugar alcohol obtained by hydrogenation of xylose is xylitol.

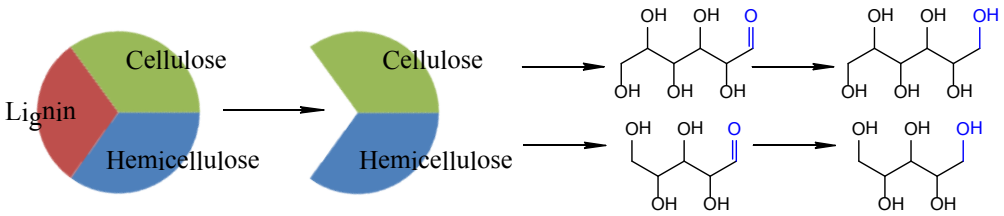

Fig. 1. Production of sorbitol and xylitol from biomass.

Thus, the two most abundant polyols are sorbitol and xylitol. According to the National Institute of Starch, the annual production of sorbitol and xylitol is 800 000 Mt and 200 000 Mt, respectively[12]. Therefore, the availability of natural and renewable sources for sorbitol and xylitol production as well as scientific endeavor to investigate this substrate in the aqueous phase reforming process encouraged our studies.

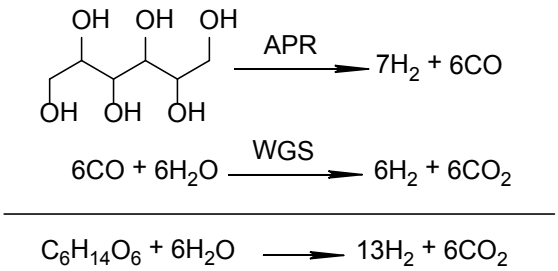

Fig. 2. Aqueous-phase reforming of sorbitol.

Aqueous-phase reforming, first introduced in 2002 by Dumesic and co-workers[13], is a catalytic transformation of biomass-derived oxygenates which allows production of both hydrogen[14] and hydrocarbons[15]. Oxygenated compounds such as sugars (glucose), sugar alcohols (sorbitol) and polyols (ethylene glycol (EG) and glycerol) can be converted into H_2, CO_2 and a mixture of alkanes

via the APR process as shown in Fig. 2. In the first step, the oxygenated substrate is transformed into H_2 and CO. Carbon monoxide reacts further with water presented in excess in the system via water-gas shift (WGS) reaction to produce more hydrogen and CO_2 as shown in Fig. 2.

Typically, the reaction is carried out over metal supported catalysts at elevated temperatures (210-250°C) and pressures (30-50 bar) in the absence[13,16] or presence of hydrogen[17,18]. In a case of hydrogen co-feeding together with the substrate solution, the process is called aqueous-phase dehydration-hydrogenation (APD/H). Different metal supported catalysts can be utilized for APR[13]. Various metals (Pt, Ni, Pd, Rh, Ru, Ir as well as alloys PtRe, PtNi, NiPd, etc) and support materials, have been screened and so far Pt is the most used and studied metal possessing the highest values of catalytic activity and selectivity towards desired products. Depending on support or reaction conditions (pH, acid additives), the reaction can be driven towards enhanced hydrogen or hydrocarbon formation. Different metal oxides (Al_2O_3, MgO, TiO_2, ZrO_2 etc.) can be used as a support for Pt particles in the APR process[13] along with zeolites[19] and carbons[20]. The number of publications available in literature devoted to aqueous-phase reforming of ethanol, ethylene glycol, glycerol, sorbitol over various catalysts has been growing significantly since 2002. Industrial feasibility of the aqueous-phase reforming process is supported by a successful process startup for APR by Virent Energy Systems[21] and developing of BioReforming Platform combining APR and conventional chemical methods for production of diesel, gasoline, jet-fuel and chemicals[22].

The aqueous-phase reforming process which might seem to be a relatively simple system as represented by Fig. 2 is in fact a very complicated process. By 2009, there were only a few contributions related to the investigation of the mechanistic aspects of this reaction[13]. In the case of C_3 substrate (glycerol), the number of products becomes ten. The detailed information on APR of higher polyols as well as experimental data on reaction products and intermediates, involved in the formation of main products was missing. It is important to note that development of novel catalytic systems and improvement of existing technologies is not possible without understanding the main reaction pathways and an understanding of kinetics aspects and optimization of the process conditions. Therefore, the main goal of the present doctoral research was a systematic investigation of aqueous-phase reforming of C_5-C_6 sugar alcohols originating from wood biomass. It was important to develop an analytical approach allowing investigating reaction products and intermediate compounds in the APR of sugar alcohols, to elucidate the main pathways of sugar alcohol transformation, to study the effect of the substrate, to optimize the catalytic system, to establish a correlation between the catalytic results and physico-chemical properties.

2. Experimental part

2.1 Chemicals

The following chemicals were purchased from commercial suppliers (Sigma-Aldrich) and utilized without further purification. The gases (H_2, mixture of 1vol. % He in N_2) were supplied by AGA Oy (purity >99.999%). Substrates: sorbitol (99.9%), xylitol (99.9%), glycerol (99%), ethanol (99.5%), chemicals for the catalyst preparation (H_2PtCl_6, $Pt(NH_3)_4(HCO_3)_2$; $Pt(NO_3)_2$ (assay 15.14%) and perrhenic acid (assay 39.4%) solutions were supplied by Johnson Matthey. Titania P90 was used as a support from Nippon Aerosil. Titanium carbide (TiC) was purchased from Goodfellow with a purity >99.8% and a mean particle size of 75 μm. Platinum precursor, $[Pt(NH_3)_4]Cl_2$ was purchased from Alfa Aesar with a purity of 99.9%; 65 wt.% HNO_3 was purchased from AppliChem as pure acid. Deionized water (18 MΩ) was used for the preparation of the catalysts as well as for APR reaction.

2.2 Catalysts

The Pt catalysts investigated in the present work were supported on different metal oxides, such as Al_2O_3 [**I-III**], TiO_2 [**IV**], MgAl mixed oxides[23] and different carbon supports [**V**].

The $PtAl_2O_3$ (F 214 XSP) and Pt/C (F 1525 XKT/W) catalysts were supplied by Degussa. The Pt catalyst supported on a carbide-derived carbon obtained by chlorination of TiC is denoted as Pt/TiC-CDC. The platinum catalysts supported on birch-active carbon Pt/BAC. Platinum was deposited on carbon support Sibunit and prepared from H_2PtCl_6 and $Pt(NH_3)_4(HCO_3)_2$ as a source of Pt denoted as Pt/Sibunit (1) and Pt/Sibunit (2), respectively. Detailed descriptions of the catalyst preparation supported on titania and carboneous materials can be found in the publication [**IV,V**].

2.3 Catalyst characterization

The catalysts were characterized by manifold techniques in order to investigate the physico-chemical properties and to establish correlations with catalytic data.

Thus, impulse CO chemisorption was applied to determine the average Pt cluster size as well as metal dispersion [**I**] (Micromeritics, Autochem 2900). The catalysts were reduced prior to the measurement according to the following program: 25–50°C at 5°C×min^{-1} in He, dwell for 30 min, gas-switch to H_2, 5°C×min^{-1} to 250°C, dwell for 2 h, followed by flushing for 60 min in He at 250°C to remove surface hydrogen. Thereafter the catalyst was cooled to ambient temperature and

CO pulses were introduced utilizing 10 vol. % CO in He. In the interpretation of the data, a Pt/CO stoichiometry of 1:1 is assumed.

Surface area measurements were performed by low-temperature N_2 physisorption [**IV,V**]. For determination of the specific surface area, BET equation (Pt/Al_2O_3, Pt-, Re-, Pt-Re/TiO_2, Pt/TiC-CDC, Pt/Sibunit 1 and 2) and Dubinin equation for microporous carbons were applied (Pt/BAC, Pt/C (Degussa)).

Temperature-programmed reduction [**I,IV,V**] was used to determine the corresponding reduction temperature for the catalysts by the AutoChem 2900 instrument. The following program was applied: $5°C \times min^{-1} \rightarrow 400°C$. The TPR was measured by placing approximately 0.1 g of catalyst in a U-shaped tube which was cooled to 25°C in Ar. The catalyst was reduced using 5% H_2 in Ar with the temperature being ramped from 25°C to 400°C (or 800°C for Pt-Re and Re samples) at a rate of $5°C \times min^{-1}$ and the hydrogen uptake monitored by a thermal conductivity detector (TCD)

Temperature-programmed desorption of NH_3 [**IV**,**V**] was performed using Micromeritics Autochem 2910 apparatus to determine the acid properties of the catalysts. Prior to the NH_3 treatment, the catalyst sample (0.1 g) was dried in an oven at 100°C overnight. The sample was then placed in a U-shape quartz tube and reduced under hydrogen flow (20 $ml \times min^{-1}$) using the following procedure: $5°C \times min^{-1}$ to 250°C, dwell for 2 h. The catalyst was then flushed in a flow of He (20 $ml \times min^{-1}$) for 30 min to remove hydrogen from the catalyst surface. The sample was cooled down to ambient temperature and saturated with NH_3 (gas mixture 5% of NH_3 in He) for 1 h. The gas mixture was then switched back to He and the catalyst was flushed for 30 min to remove physically adsorbed ammonia. Temperature-programmed desorption was performed in the temperature interval of 25-225°C at various heating rates (3, 5, 10, 15, 20 $°C \times min^{-1}$). After each cycle, the catalyst was treated by a mixture of ammonia in helium prior to the TPD measurements as described above. Ammonia desorption was monitored by the changes in the TCD signal. Heat of desorption was calculated with a standard approach which includes plotting T_p (temperature at maximum of desorption in K) versus $\ln (T_p^2/\beta)$ (where β corresponds to a heating rate) followed by calculation of the slope, and then E_{des} [$kJ \times mol^{-1}$]. The number of acid sites for each catalyst was counted as the amount of ammonia desorbed upon heating at $3°C \times min^{-1}$. The values are reported as the amount of NH_3 desorbed per catalyst weight. The TPD graphs are presented in K.

High-resolution transmission electron microscopy (TEM) [**V**] was performed with LEO 912 Omega, voltage 120 kV. The samples for TEM were prepared as a suspension in ethanol and for calculating the diameter of particles; ca. 500 particles for each sample were taken.

In situ liquid phase XANES (X-ray absorption near edge spectroscopy) [**IV**] was performed (for Pt, Re and Pt-Re samples[24]) of the CenTACat School of Chemistry at Queen's University of Belfast (UK) in a homemade cell comprised of a stainless steel autoclave reactor with an opening (cut window) and a PEEK (polyether ether ketone) inlet. The detailed experimental procedure is described by Hardacre and co-workers[24].

2.4 Reaction procedure

For the APR studies reported in the present study, a continuous fixed-bed reactor setup (stainless steel reactor, $d = 4.8$ mm, $l = 18$ cm) equipped with a furnace was used. The reactor setup is shown in Fig. 3. In a standard experiment, the catalyst (0.5 g) was mixed with ca. 3 g of quartz sand and loaded to the reactor. The catalyst was reduced prior to the measurements with H_2 using the following program: 25→ 250°C at 5°C×min^{-1} in H_2 for 2 hours, at a H_2 flow rate of 30 ml×min^{-1}.

The reaction was carried out at 225°C and 29.3 bar, at a range of space velocities of 0.9 – 6.0 h^{-1}. Weight hour space velocity (WHSV) is defined as mass of substrate fed per mass of the catalyst per hour [$g_{sub} \cdot g_{cat}^{-1} \cdot h^{-1}$]. An aqueous solution (10 wt. %) of substrate (sorbitol, xylitol, glycerol or ethanol) was fed continuously via an HPLC pump.

Regeneration procedure for Pt/Al_2O_3 catalyst: $PtAl_2O_3$ was regenerated to recover the catalytic activity after approximately 120 h time-on-stream. The procedure comprised washing the catalyst with acetone followed by reduction in hydrogen flow under conditions described above.

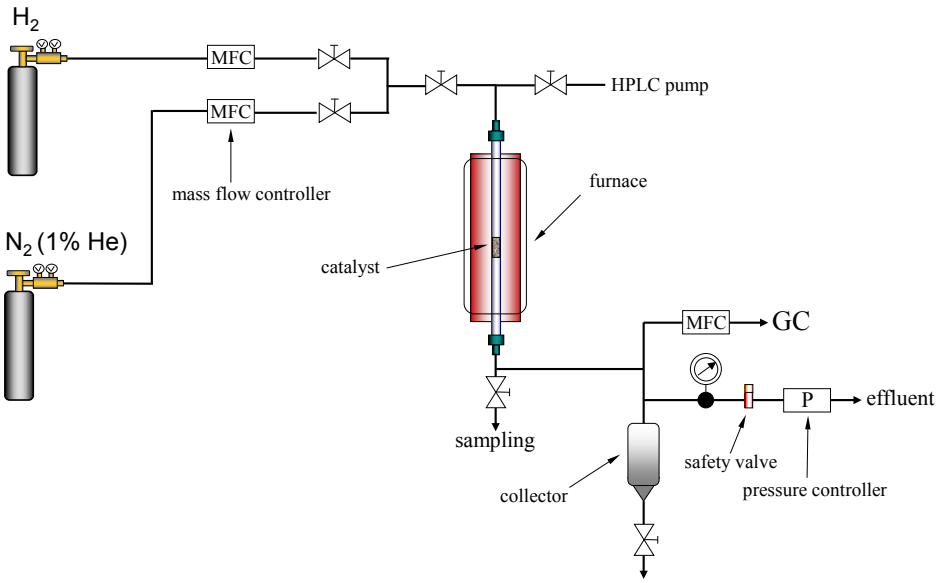

Fig. 3. Scheme of the reactor setup for aqueous-phase reforming of sugar alcohols.

2.5 Analysis of reaction products

Liquid samples were taken periodically and analyzed by means of high-performance liquid chromatography (HPLC), applying an injection volume 2 µl, Aminex HPX-87H column, eluent 5mM H_2SO_4, flow rate 0.6 ml×min^{-1}, 45°C, 70 min) applying a refractive index (RI) detector to determine the xylitol conversion.

Gaseous products were analyzed periodically by means of a micro-GC (Agilent Micro GC 3000A). The instrument was equipped with four columns: Plot U, OV-1, Alumina and Molsieve. The micro-GC was calibrated to perform quantitative analysis for the following gases: H_2, CO_2, CO, CH_4, linear hydrocarbons C_1-C_4 and 1 wt.% of He in N_2 was used as an internal standard. Moreover, the carbon balance was monitored by means of total organic carbon analysis (TOC-5050 analyzer (Shimadzu)) and was confirmed to a degree of 95-100% for all the measurements.

2.6 Calculation of yields, selectivities and catalyst activity

The turnover frequencies (TOF) for Pt and Pt-Re supported catalysts were calculated using the following equation for hydrogen:

$$TOF[\min^{-1}] = \frac{r(H_2)[mol \cdot \min^{-1}]}{\nu(M)\,[mol] \cdot D\,[a.u.]} \quad (1)$$

where r(H_2) denotes the rate of H_2 formation, υ(M) –moles of Pt and D – dispersion (determined by CO chemisorption), and for alkanes

$$TOF[\min^{-1}] = \frac{r(alk)[mol \cdot \min^{-1}]}{\nu(M)\,[mol] \cdot D\,[a.u.]} \quad (2)$$

where r(alk) denotes the rate of the total alkane formation in the gas phase, υ(M) –moles of Pt and D – dispersion (determined by CO chemisorption).

The yield and selectivity to H_2 for the APR process were calculated as follows[13]:

$$\text{Yield of } H_2\ (\%) = \frac{r(H_2)}{V(subst) \cdot 0.1/M \cdot R} \times 100\% \quad (3)$$

where r(H_2) – rate of hydrogen production (mol×min^{-1}), $V_{(subst)}$ – solution feed rate (ml×min^{-1}), M – substrate molar mass, R – stoichiometric coefficient of H_2 formation (11 - for xylitol, 13 – for sorbitol).

$$\text{The selectivity to hydrogen is } S_{H2}(\%) = \frac{\nu(H_2)}{\nu(C_{in\ gas})} \times 1/RR \times 100\% \quad (4)$$

where $\nu(H_2)$ – moles of H_2 formed, $\nu(C_{in\ gas})$ – moles of carbon in gas, RR – H_2/CO_2 reforming ratio (13/6 for sorbitol, 11/5 for xylitol, 7/3 for glycerol).

$$\text{The selectivity to alkanes is } S_{alk}(\%) = \frac{\nu(C_{alkanes})}{\nu(C_{in\ gas})} \times 100\% \quad (5)$$

where $\nu(C_{alkanes})$ – moles of carbon in alkanes and $\nu(C_{in\ gas})$ – total moles of carbon in gas.

The hydrogen yield and selectivity to hydrogen and alkanes were calculated in non-conventional manner per amount of carbon in gas $C_{in\ gas}$ in order to compare the results with data reported in literature.

3. Results and discussion

3.1 Catalyst characterization

The following Pt supported catalysts were selected and examined in APR of polyols within the framework of this doctoral research: Pt/Al_2O_3, Pt/TiO_2, $Pt\text{-}Re/TiO_2$, Re/TiO_2, Pt/TiC-CDC, Pt/AC (Degussa), Pt/BAC, Pt/Sibunit.

The textural properties of the catalysts are summarized in Table 1.

Table 1. Texture and surface properties of the Pt catalysts

Catalyst	**Metal, content,** %	**Surface area,** $m^2 \times g^{-1}$	**Pore volume,** $cm^3 \times g^{-1}$	**Pore diameter,** nm	**CO uptake,** $\mu mol \times g^{-1}$	**CO/(total M) atomic ratio**	**d(Pt) by chem.,** nm	**d(Pt) by TEM,** nm
Pt/Al_2O_3	5	110	0.25	8.2	74.6	0.29	3.9	-
Pt/TiO_2	4	83	0.20	-	49.1	0.24	4.7	-
$Pt\text{-}Re/TiO_2$	4-4	53	0.17	-	103.1	0.25	5.0	-
$Re\text{-}TiO_2$	4	63	0.22	-	59.8	0.29	-	-
Pt/TiC-CDC	2.8	850	0.61	1.4	18.3	0.12	9.0	3.3±1.0
Pt/C (Degussa)	5	910	0.52	1.5	119.6	0.47	2.4	2.8±1.0
Pt/Sibunit (1)[a]	5	339	0.53	2.9	31.3	0..12	9.0	3.4±0.6
Pt/Sibunit (2)[b]	5	408	0.47	2.6	104.5	0.41	2.8	1.9±2.1
Pt/BAC	5	890	0.45	1.2	191.5	0.29	1.5	2.0±1.8

[a]- Pt/Sibunit (1) – corresponds to the Pt/Sibunit prepared from $(NH_3)_4Pt(HCO_3)_2$.
[b]- Pt/Sibunit (2) – corresponds to the Pt/Sibunit prepared from H_2PtCl_6,

The catalysts have Pt loadings between 2.8 and 5 wt.% as can be seen from Table 1. All materials are nanoscale supported catalysts with the average size of Pt below 10 nm. Dispersion of the catalysts was determined by two different techniques: pulse CO chemisorption and TEM. The TEM images along with the particle size distributions are depicted on Fig. 4. In general, both techniques showed a good correspondence in terms of the Pt cluster size determination. However, some discrepancy in the results was obtained for samples Pt/TiC-CDC and Pt/Sibunit (1). The plausible reason for that might be the fact that during TEM imaging only selected parts of the catalytic material were exposed to examination, not representing therefore the whole particle size distribution. As for the case of Pt/Sibunit (1), the discrepancy was caused in our opinion by the partial melting of the Pt particle into the background which in turn complicated the identification of metal particles and corresponding size distributions (Fig. 4e) [**V**].

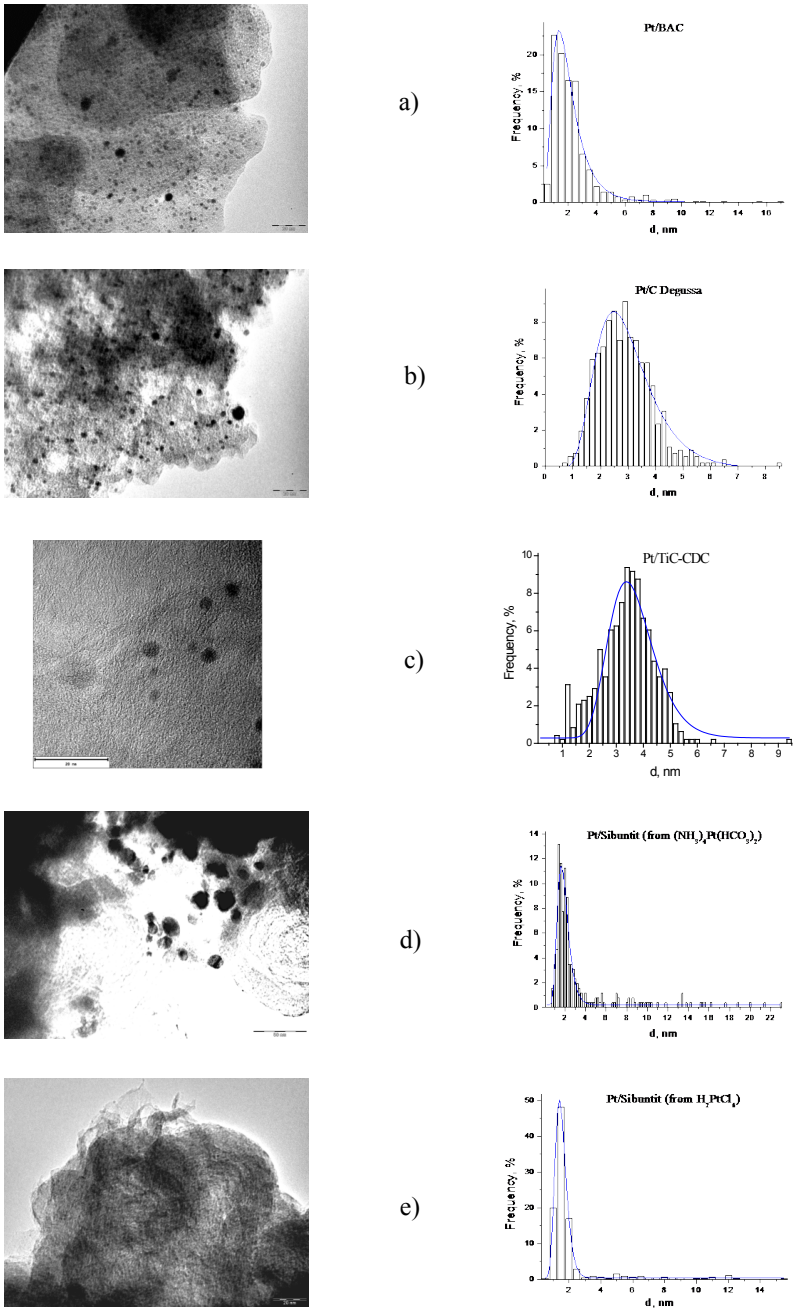

Fig. 4. TEM image and corresponding particle size distribution of a) Pt/BAC b) Pt/AC (Degussa), c) Pt/TiC-CDC, d) Pt/Sibunit (1) and Pt/Sibunit (2) catalysts.

It is important to note that for all the catalysts examined by TEM, a narrow monomodal particle size distribution was observed.

The catalysts were subjected to temperature programmed reduction (TPR) under hydrogen flow to determine the corresponding reduction temperatures. The TPR profiles for the catalysts are shown on Fig. 5.

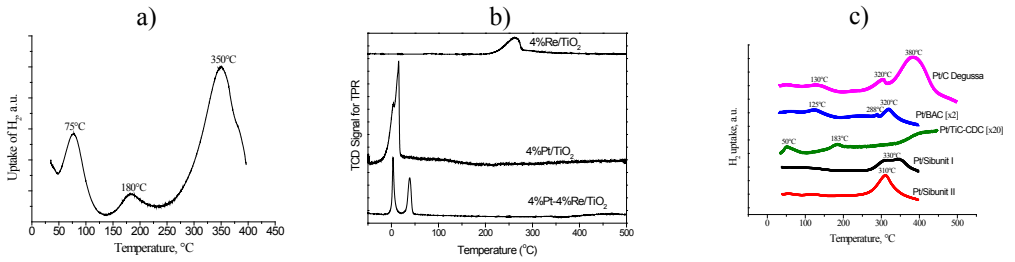

Fig. 5. TPR profiles for a) Pt/Al_2O_3 [**I,III**], b) Pt/TiO_2, $Pt\text{-}Re/TiO_2$, Re/TiO_2 [**IV**] and c) series of Pt/C [**V**] catalysts.

The Pt/Al_2O_3 catalyst demonstrated three peaks in a TPR profile: at 73, 180 and 350°C. The first two peaks may be attributed to reduction of PtO_x species, whereas a high-temperature peak is most likely caused by the interaction of Pt with the Al_2O_3 support[25]. The Pt/TiO_2 catalyst demonstrated two low temperature peaks of hydrogen uptake (below 100°C) and one at 300-350°C as evidenced from the TPR profile shown on Fig. 5b. The TPR analysis of the 4 wt.% Pt – 4 wt.% Re/TiO_2 catalyst showed three peaks at 3°C, 40°C, and 400–600°C[26]. The first two peaks correspond to the reduction of Pt only, in agreement with the TPR of the 4 wt.% Pt/TiO_2 catalyst, and to oxygen at the interface between Pt and Re, indicating significant interactions between Pt and Re. High temperature peaks at 315°C and 380°C were found for 4 wt.% Re/TiO_2[26]. These high temperature peaks could be due to the reduction of ReO_x[27] and/or reduction of the bulk titania support.

The Pt/C catalysts after preparation were reduced using various techniques. The detailed data are provided in the experimental section in article [**V**]. However, as can be seen from the TPR curves, formation of Pt oxide species might occur. The high temperature hydrogen consumption peaks above 300°C can be assigned to hydrogen spill-over. The hydrogen uptake was very low in the case of Pt/BAC, since this catalyst was reduced chemically by HCOOH. During storage, the catalytic material is partially oxidized as revealed by the TPR curve: the peak at 125°C corresponds to the reduction of PtO_x species.

Table 2. Acidic properties of Pt supported catalysts

Catalyst	NH_3 desorbed*, µmol×g^{-1}	E_{des} (NH_3), kJ×mol^{-1}
Pt/Al_2O_3	317	52
Pt/TiO_2	279	47
$Pt\text{-}Re/TiO_2$	220	68
$Re\text{-}TiO_2$	-	-
Pt/TiC-CDC	6	45
Pt/C (Degussa)	47	51
Pt/Sibunit (1)[a]	103	53
Pt/Sibunit (2)[b]	92	54
Pt/BAC	158	51

[a]- Pt/Sibunit (1) – corresponds to the Pt/Sibunit prepared from $(NH_3)_4Pt(HCO_3)_2$. [b]- Pt/Sibunit (2) – corresponds to the Pt/Sibunit prepared from H_2PtCl_6,

Prior to all the tests, the catalysts were pre-reduced under hydrogen flow for 2 hours at 250°C. Therefore, treatment at 260°C for 2 hours under hydrogen flow leads to a complete reduction of Pt. Thus, the Pt oxidation state for all the Pt supported catalysts can be regarded as Pt(0).

The acidic properties of the Pt catalysts were evaluated by temperature-programmed desorption of ammonia. The data are collected in Table 2.

The detailed data on acidity measurements and corresponding NH_3-TPD profiles are reported in [**IV**] and [**V**] for Pt/MO_x and Pt/C, respectively. The NH_3-TPD profile for Pt/Al_2O_3, shown as an example, exhibited a peak at 349-386 K, depending on the heating rate (Fig. 6a). Desorption of ammonia at these temperatures implies a weak interaction of NH_3 and acid sites of the catalyst being mainly physisorption rather than acid-base interaction. Thus, Pt/Al_2O_3 is a catalyst with a low acidity and does not contain, according to NH_3-TPD data, strong and medium strength acid sites. Moreover, the calculated heat of desorption is 52 kJ×mol^{-1} is a very low value corresponding to a weak interaction of ammonia and acid sites of the support (Fig. 6b).

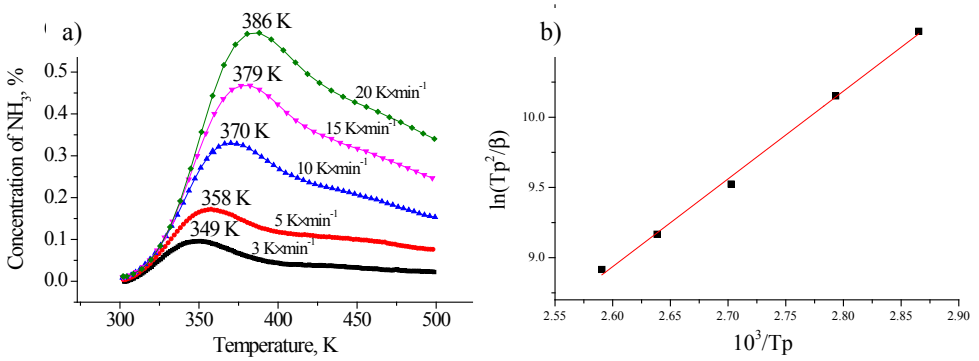

Fig. 6. Determination of acidity for Pt/Al_2O_3 by NH_3-TPD (a) and calculation of E_{des} (b) [**IV**].

The NH_3-desorption curves were recorded for all the catalysts investigated in the present work. Quantitative data on acidity are given in Table 2. As can be seen, the higher values of acidity were observed for catalysts supported on metal oxides, whereas Pt/C possessed a moderate amount of acidic sites capable of adsorbing ammonia molecules in the range of 6-158 μmol×g^{-1}. Pt/Al_2O_3 demonstrated a higher acidity compared to the samples supported on TiO_2. In addition to a significant impact on acidic properties of the material[28] by addition of Re, it leads to formation of stronger acid sites on the catalyst surface. However, the total number of acid sites is diminished after addition of Re as can be noticed from Table 2. The acidities of the Pt/C catalysts decrease in the following order: Pt/BAC > Pt/Sibunit (2) > Pt/Sibunit (1) > Pt/C (Degussa) > Pt/TiC- CDC. Generally speaking, the surface acidity of carbon materials is determined by the surface chemistry of the carbons, i.e. by the functional groups presented on the carbon surface[29]. The fact that some catalyst materials exhibiting higher values of E_{des} possessing less number of acid sites is explained by the difference in the nature of the carbon material, Pt source as well as a catalyst preparation technique.

3.2 Mass transfer effects

Prior to obtaining the experimental catalytic data, the absence of external and internal diffusion limitations was checked for the APR of sorbitol. In order to study the influence of external mass transfer limitations, a series of experiments was performed at different contact times (Fig. 7). The linear dependence of the conversion versus contact time reflects the absence of external mass transfer limitations.

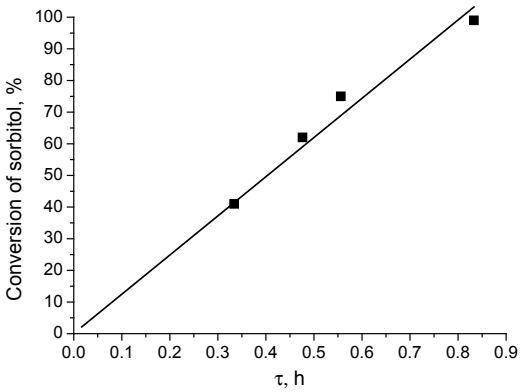

Fig. 7. Dependence of the substrate conversion on contact time between the substrate and the catalyst [**VI**]..

In order to verify the absence of internal diffusion limitations the Weisz-Prater criterion was used[30]. Due to this criterion no pore diffusion limitation occurs, if the Weisz-Prater modulus

$$\Phi = \frac{r_{obs} R^2}{c D_{eff}} \qquad (6)$$

for the first order reaction is below unity ($\Phi < 1$), for zero order reaction $\Phi < 6$ and for the second order reaction the modulus is below 0.3. In equation (6) r_{obs} — maximal initial reaction rate, R —

the mean radius of the catalyst particle, c — the substrate concentration. The largest radius of the Pt/Al_2O_3 catalyst particle is 1.25×10^{-4} m (125 μm).

The effective diffusion coefficient (D_{eff}) of substrate (sorbitol) in water is defined as $D_{ef} = D\frac{\xi}{\chi}$, where D is the substrate diffusion coefficient in the liquid phase, ξ χ are catalyst porosity and tortuosity, respectively. Typical values of porosity are in the range 0.3-0.6, while values of tortuosity are varied from 2 to 5.

Equation of Wilke-Chang was used for calculation of the molecular diffusion coefficient:

$$D^{o}_{AB} = \frac{7.4\times10^{-8}(\phi\, M_B)^{1/2}T}{\eta_B\, V_{b(A)}^{0.6}}\ [\mathrm{cm^2/s}] \qquad (7)$$

The dimensionless association factor ϕ is taken 2.6 for water, M_B is the molecular weight of solvent, η_B = 0.11888 cP is solvent dynamic viscosity at reaction temperature T (K) and pressure (estimated at 498 K and 30 bar), $V_{b(A)}$ = 122.15 $cm^3\times mol^{-1}$ is the liquid molar volume at solute's normal boiling point. Assuming ξ/χ = 1/10 the diffusion coefficient of sorbitol is calculated to be D_{ef} =1.18×10^{-9} m^2/s (498 K and 30 bar). The concentration of the substrate in the solvent is equal to 0.515 $mol\times l^{-1}$. For the maximal sorbitol reforming rate (1.93×10^{-4} $mol\times l^{-1}\times s^{-1}$ calculated at 2.7 h^{-1} [**III**]) obtained for the Pt/Al_2O_3 catalyst the estimated Weisz-Prater modulus was amounted to Φ=0.005. It indicates that substrate diffusion inside the catalyst pores does not affect the reaction rate.

3.3 Catalyst stability studies

All the catalysts described in the present work were subjected to long-run stability tests to investigate possible deactivation. As for example, Fig. 8 displays time-on-stream changes in conversion and selectivity to hydrogen of two Pt supported catalysts in the APR of xylitol.

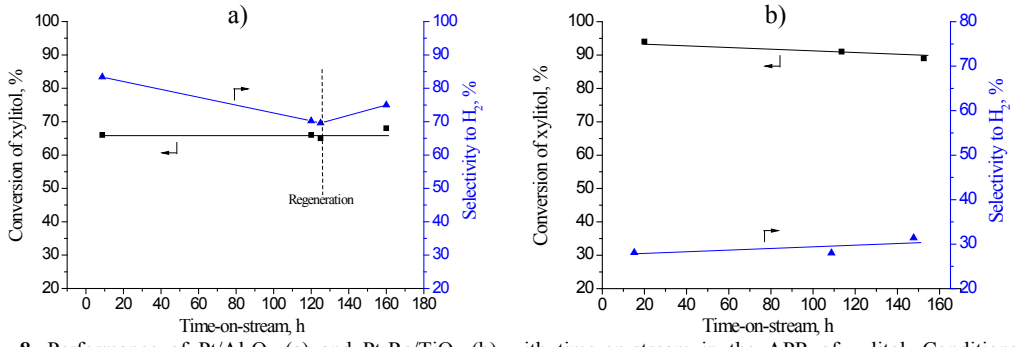

Fig. 8. Performance of Pt/Al_2O_3 (a) and $Pt\text{-}Re/TiO_2$ (b) with time-on-stream in the APR of xylitol. Conditions: Conditions: 225°C, 29.3 bar, 10 wt.% xylitol solution, 30 $ml\times min^{-1}$ nitrogen flow rate, 1.8 h^{-1} [**III,IV**].

The Pt supported catalysts demonstrated a stable performance within more than 140 h time-on-stream [**I, III**]. Minor deactivation expressed by decrease in selectivity to hydrogen was observed in a case of Pt/Al_2O_3. However, the catalyst may be subjected to a regeneration procedure (see Experimental part for details) and the selectivity towards the desired product may be regained. In the article [**III**] we explain the change in the selectivity towards hydrogen by the fact that during aqueous-phase reforming under severe hydrothermal conditions, γ-Al_2O_3 might transform into boehmite. In fact, the transformation of unsupported γ-Al_2O_3 into boehmite is completed within 10 hours under similar experimental conditions; however, the presence of Pt leads to an increase of the hydrothermal stability of the material and retards this transformation process as stated by Ravenelle *et. al.*[31]. Furthermore, as shown recently by the same research group[32], the presence of a polyol substrate (sorbitol, glycerol) significantly reduces the boehmite formation compared to hot water. Moreover, the stabilizing effect was even more profound in the case of sorbitol compared to glycerol. It is concluded[32] that higher stability in the presence of polyol substrates was due to formation of protective carboneous layer containing different functional groups which prevents formation of boehmite. On the other hand, the deposition of carboneous layer led to a significant blockage of the metal surface area. Therefore, during APR of xylitol, formation of carboneous layers might take place thus stabilizing the catalytic material: as can be seen, the conversion does not change with time-on-stream (TOS). Nevertheless, the blockage of the metal surface area might lead to the decrease in hydrogen selectivity. The fact that regeneration procedure indeed helped to regain the selectivity implies that washing of the catalyst layer with acetone followed by reduction in hydrogen flow at 225°C partially removes adsorbed carboneous species rescuing the metal surface area which in turn leads to the improvement in selectivity.

Bimetallic Pt-Re sample supported on TiO_2 showed insignificant deactivation (less than 5% within 150 h TOS) [**IV**]. All the catalysts supported on carbons demonstrated high stability during long-run tests. For example, changes in conversion of xylitol and selectivity to hydrogen were within 10% after 120 h performance of Pt/TiC-CDC with time-on-stream. Other Pt/C catalysts also demonstrated a stable behavior without any noticeable deactivation [**V**].

3.4 Identification of reaction products [I]

The main products which are formed during aqueous-phase reforming of sorbitol are H_2, CO_2, and a mixture of alkanes in the gas phase as well as oxygenated products which are mainly present in the liquid phase (Fig. 9). As has been mentioned earlier, transformations of the initial polyol result in

formation of H_2 and CO at the first step. Carbon monoxide is then converted via water-gas-shift reaction which takes place under the similar experimental conditions to form CO_2 and additional hydrogen molecules[16]. However, hydrogen formed may be involved in side hydrogenation processes of C=C or C=O bonds as well as hydrogenolysis reactions leading to its consumption and formation of hydrogenated intermediates. The gaseous products were collected in bottles and further analyzed by means of micro-GC and GC-MS. Therefore, the analysis of gas-phase products revealed formation of C_2-C_6 alkanes in the gaseous phase. The concentration of hexane, however, was very low. It is important to note that CO did not appear among the reaction product (which in fact means that its concentration is below the detection limit by micro-GC being~100 ppm). Total organic carbon analysis was applied to monitor the carbon balance during the APR reactions. In all the experiments, the carbon balance was 95-100%.

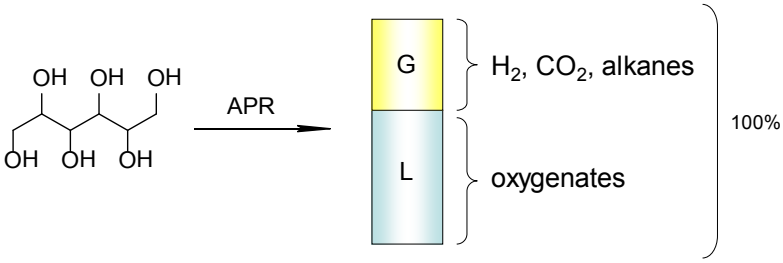

Fig .9. Distribution of products between gas and liquid phases in the APR of sorbitol.

In order to investigate the type and structure of intermediates formed as well as structure of liquid-phase products, an approach comprising up-to-date analytical methods was developed and applied. The schematic representation of the method is shown in Fig. 10. To identify the volatile compounds, the solid-phase micro-extraction method was used (SPME). In brief, the method includes adsorption of volatiles by the carbon polymer coated fiber followed by GC-MS analysis of the adsorbed molecules[33]. Enormously large amount of products (> 260) can be formed during the APR of sorbitol [**I**] as has been shown by GC-MS, HPLC and SPME.

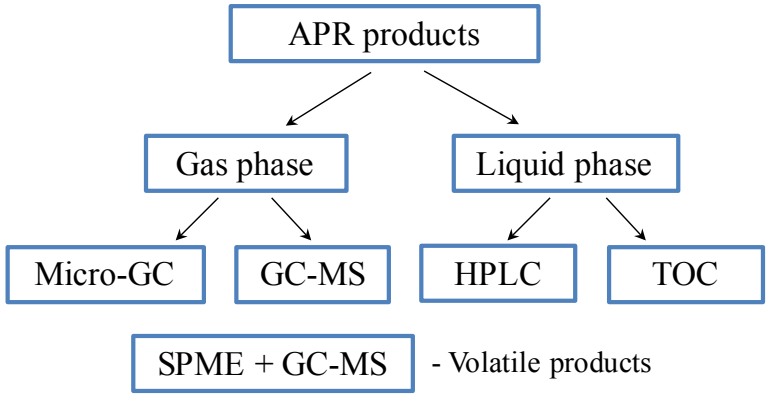

Fig. 10. The scheme representing analytical tools applied to investigation of reaction prodcuts in the APR of sorbitol.

However, the concentrations of most of these products were negligible; therefore, 25-30 main components might be selected and considered as reaction intermediates and products. They include mainly ketones, alcohols, furanes, cyclic ethers, carboxylic acids, etc [**I**]. The composition of the reaction mixture as well as pathways of products formation will be discussed below.

3.5 Aqueous-phase reforming of sugar alcohols: effect of the substrate structure [II,III]

As mentioned above, aqueous phase reforming of polyols results in formation of hydrogen and CO_2 as the main products in the gas phase. Additionally, a mixture of hydrocarbons is also formed.

Typical curves illustrating conversion of the initial substrate and selectivity to hydrogen are shown on Fig, 11.

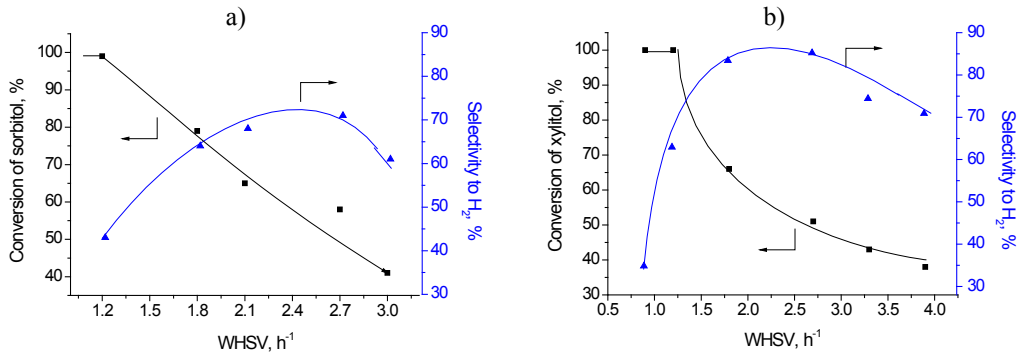

Fig. 11. Conversion of the substrate and selectivity to H_2 as a function of space velocity [**III**]: a) sorbitol, b) xylitol [**III**].

As can be seen, the conversion decreases for both substrates as WHSV increases. This is caused by shorter contact times between the catalyst and the feed at higher values of space velocity. Hydrogen formed during the APR process is inevitably involved in side-reactions such as hydrogenolysis of the initial substrate or hydrogenation of dehydrated intermediates, which contributes to its consumption and results in a lower selectivity towards hydrogen.

Moreover, hydrogen which is formed during APR of xylitol may be consumed in hydrogenolysis of C-C and C-O bonds of the initial substrate and intermediate compounds. These reactions considerably lowered the yield and selectivity of APR process towards hydrogen in the case of sorbitol [**I**].

At lower space velocities, the contact time of the feed and the catalyst in hydrogen rich conditions is higher. Therefore, hydrogen consuming reactions contribute to a larger extent and depletion in the

selectivity is observed. This explanation is in perfect correlation with previous experimental results of Huber and Li obtained for APD/H process[17].

The higher selectivity observed for the substrate with a shorter carbon chain can be attributed to the lower probability of side-reactions because hydrogen which is formed participates in many different side-reactions. Such a tendency was also observed for the following sequence: methanol – ethyleneglycol – glycerol – sorbitol[13] wherein the yield of H_2 increased as follows:

$$\text{sorbitol} < \text{glycerol} < \text{ethyleneglycol} < \text{methanol},$$

thus highlighting that the substrates bearing less carbon atoms in a chain are more selective in terms of hydrogen production. Moreover, higher rates of hydrogen production were earlier observed for glycerol in comparison to sorbitol [**II**]. Similar trends have been observed over Pt-Re/C catalysts; therefore, the selectivity and hydrogen yield depend on the nature of the substrate[34].

Generally, the yield of H_2 increases with a decrease in WHSV and goes through a maximum in both cases [**III**]. The yield of H_2 is higher for xylitol throughout the range of the space velocities studied. Thus, the highest yield corresponding to 32% was observed for xylitol at 1.8 h^{-1}, while the maximum yield for sorbitol was 21%, at the same space velocity.

During APR, mainly formation of linear alkanes was observed. In general, the alkanes comprised ethane, propane, *n*-butane and *n*-pentane in the case of xylitol [**III**].

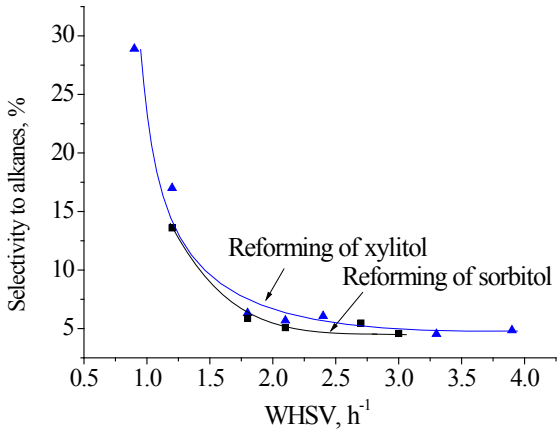

Fig. 12. Comparison of selectivities to alkanes in APR of sorbitol and xylitol [**III**].

Trace amounts (<0.1%) of *n*-hexane were detected in the case of sorbitol [**I,III**]. Selectivity profiles for both substrates are shown in Fig. 12.

It can be seen that, in both cases, the selectivity to alkanes decreases with an increase in space velocity. These data coincide well with the data on H_2 selectivity (Fig. 11). Obviously, hydrogen is involved in the formation of alkanes from oxygenated substrates as also reported in earlier studies[16]. Therefore, formation of alkanes at lower values of WHSV is favored, explaining the higher alkane selectivity.

Depending on the space velocity, the distribution of carbon presented initially in the substrate varied. The carbon content in the gas phase increases with an increase in contact time between the catalyst and the feed. Therefore, the amount of carbon-containing products is higher at higher substrate conversions. This tendency is valid for all the substrates investigated and for all the catalytic systems.

As has been mentioned above, the liquids-phase product formation takes place during APR of polyols. The detailed study on the composition of liquids phase in the aqueous phase reforming of sorbitol is reported in [**I**]. It is important to note that similar composition of the liquids phase mixture has also been observed for the APD/H process of sorbitol by Li and Huber[17].

The composition of the liquid phase in APR of xylitol, at 0.9 h^{-1}, is depicted in Fig. 13.

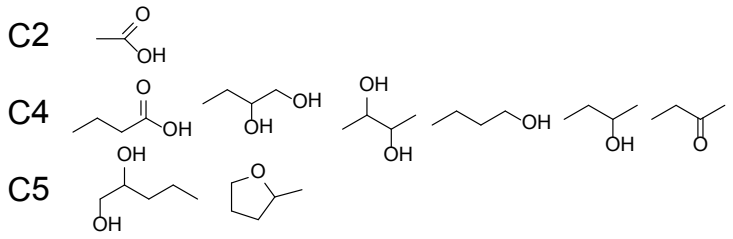

Fig. 13. Composition of the liquid phase in APR of xylitol. 95% of all compound present in the liquid phase are detected. Carbon content in the liquid phase is 14% [**III**].

It was possible to identify 70-90% of the liquid phase products in the APR of sorbitol [**I**], while for xylitol up to 95% of compounds presented in the liquid phase were detected [**III**]. A comparison of the liquid phase composition is given in Table 3.

Table 3. Liquid phase composition for APR of xylitol and sorbitol at0.9 h^{-1} [**I, III**].

Substrate	Carbon in liquid phase, %	Product distribution,%						Total products detected, %
		alcohols	diols	ethers	ketones	acids	other products	
Xylitol	13.2	16.4	27.2	7.0	1.6	36.8	11.0	89.0
Sorbitol	24.4	17.3	49.9	4.2	5.0	4.9	18.7	81.3

It can be seen, that the liquid phase is composed mainly of mono- and bifunctional products including linear alcohols, diols, ethers, ketones and acids. At the long contact times and therefore at complete conversion of xylitol, most of the carbon is presented in the gas phase. Meanwhile, only thermodynamically stable compounds which do not further undergo transformations are present in the liquid phase under these experimental conditions. Under the sane experimental conditions, more carbon stays in the liquid phase in the case of sorbitol compared to xylitol. The composition of liquid phase is similar in xylitol and sorbitol APR. However, in the case of xylitol a significantly lower amount of diols was formed compared to sorbitol. On the other hand, during APR of sorbitol, the amount of carboxylic acids detected in the reaction mixture was 4.9%, whereas for the case of xylitol, the amount was substantially higher – 36.8%.

On the basis of the experimental data obtained from reforming of sorbitol [**I,III**[and xylitol [**III**], the analysis of the selectivities towards the main products (H_2, CO_2, alkanes) and consideration of the liquid phase composition, the advanced scheme describing the main pathways of polyols transformations under APR conditions was proposed (Fig. 14).

Moreover, the scheme proposed takes into account the results obtained earlier by other research groups on elucidation of the reaction pathways of polyols[16,17,35].

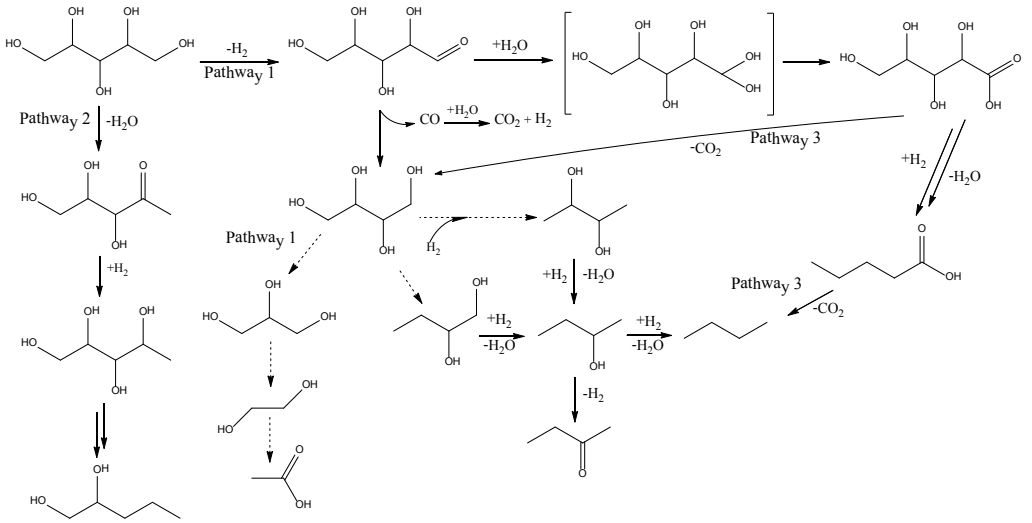

Fig. 14. The main pathways of xylitol transformation during aqueous-phase reforming [**III**].

Degradation of the initial substrate may occur via various routes as recently was reported for glycerol[35]. However, the number of possible processes involving metal and acid sites of the catalytic material thereby influencing the intermediate formation in the case of C_5 and C_6 polyol species is much higher compared to glycerol. Generally speaking the formation of the same intermediates, for instance, carboxylic acids can proceed via different routes. We have reported previously that initially a molecule can undergo dehydrogenation on the metal sites leading to the formation of short-lived aldehyde species not detected in the liquid phase (Fig. 14, Pathway 1). The aldehyde species may react with water to form acetals. This reaction can proceed over acid sites of Al_2O_3. The acetal intermediate may further undergo dehydrogentaion which leads to the formation of carboxylic acid. Aldehydes can undergo decarbonylation to form polyols with shorter carbon chains as shown by Wawretz et al.[35]. Carbon monoxide eliminated during this step is converted to H_2 and CO_2 via water-gas shift reaction. Moreover, the formed H_2 may participate in the hydrogenolysis of C-C and C-O bonds either of the initial substrate or of any oxygenated intermediates[16,17,35] [**III**].

Elimination of either CO from the aldehyde intermediates (Pathway 1) or CO_2 from carboxylic group (Pathway 3) leads to the formation of polyol species with a shorter carbon chain, for instance, erythritol. This compound may undergo hydrogenolysis of the C-O bond in the presence of hydrogen on Pt, resulting in formation of less oxygenated molecules such as diols. This can be a plausible explanation for the formation of butanediols (butanediol-1,2 and butanediol-2,3) under

experimental conditions (Fig. 14). Butanediols may in turn be further hydrogenated leading to butanols (butanol-1 and butanol-2) which were also detected. Elimination of the hydroxyl function from butanols results in formation of butane which is present in the gas phase during APR of xylitol and sorbitol as discussed above. Furthermore, dehydrogenation of butanol-2 over platinum surface can be a plausible explanation for butanone-2 formation.

Erythritol being a polyol compound may be transformed via the reaction pathway 1 to glycerol and further to ethylene glycol which were both found in the reaction mixture in the liquid phase during the experiments. Formation of acetic acid, found in the liquid phase for both substrates, may follow pathways similar to butanoic acid formation.

Likewise, the initial polyol may undergo dehydration at terminal carbon atom to form carbonyl compounds (Pathway 1). Furthermore, the carbonyl group can be hydrogenated in the presence of hydrogen to form a polyol species with less oxygen atoms than in the initial polyol. Repetition of these steps can lead to formation of the final mono- or bifunctional compounds without scission of the carbon chain, such as pentanediol-1,2, which were detected in the reaction mixture (Fig. 14).

It can be assumed that the initial polyol can undergo dehydration resulting to cyclic intermediates with a carbonyl function (Fig. 15). The carbonyl group can be hydrogenated over platinum surface resulting in formation of a cyclic ether with three hydroxyl groups. Repetition of several dehydration/hydrogenation steps or cleavage of C-O bonds via hydrogenolysis on platinum clusters may lead to the formation of cyclic 2-methylpyrane. It is worth mentioning that in the presence of these compounds was confirmed in the liquid phase in APR of xylitol at 0.9 h^{-1}.

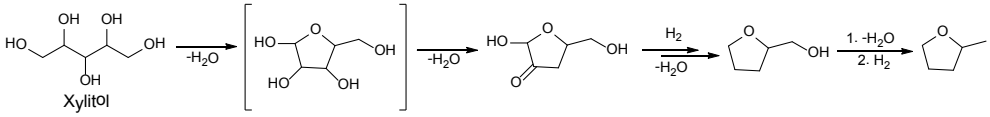

Fig. 15. Formation of 2-methyltetrahydrofuran during APR of xylitol [**III**].

Meanwhile, the substrate – xylitol – may undergo dehydration on the terminal position to form enol leading to a ketone which can be hydrogenated further on the platinum surface to a corresponding alcohol which in turn can undergo further transformations. In the APR of C_5-C_6 polyols, the contribution of other reactions such as retro-aldol reaction catalyzed by acidic/basic sites of the support might be significant along with various dehydration/hydrogenation processes [**I**]. The hypothesis that intermediate products can react with each other is proven by APR experiments with sorbitol-ethanol mixtures [**II**]. It was observed that addition of ethanol to sorbitol improved the

hydrogen yield and resulted in less amount of side products formed. It has been assumed that ethanol being much more reactive under APR conditions compared to sorbitol reacted with intermediate species thus enhancing the process of hydrogen formation from sorbitol.

3.6 Aqueous-phase reforming of polyols over Pt/MO_x: the effect of support properties and Re addition [IV]

Production of hydrogen and hydrocarbons from polyols via APR has bifunctional nature[16]. As has been shown previously, dehydration reactions mainly occur on acid sites of support, whereas hydrogenation and hydrogenolysis reactions take place over metallic sites. Recently Menezes et. al. has demonstrated that the nature of the catalyst support has a significant impact on hydrogen formation in APR of glycerol[36]. Guo et. al[37] also revealed that the acid-basic properties of the support substantially influence the activity of the catalytic material in terms of hydrogen production. The more basic is the catalytic support, the more the reaction is directed towards hydrogen formation. Hence, formation of hydrocarbons is supposed to be facilitated over more acidic supports. However, the supports with substantial acidic properties suffer from low stability under severe hydrothermal conditions. Therefore, additional acidity to the catalytic material can be imposed by introduction of a second metallic component. It is known that the addition of Re to Pt leads to an increase in the surface acidity of the resulting material since Re is withdrawing electron density from Pt thus forming slightly positive charge on the noble metal[38]. Moreover, PtRe alloys are probably the most important for the chemical industry[39]. Therefore, Pt supported on titania was chosen to investigate the effect of the support, and $Pt\text{-}Re/TiO_2$ catalyst was utilized to study the effect of the Re addition on the product formation in APR.

Platinum supported on titania was anticipated to demonstrate inferior performance in terms of the hydrogen formation compared to alumina supported catalyst since the basicity of this support is lower[37]. Indeed, significantly higher selectivities and yields of hydrogen were observed in

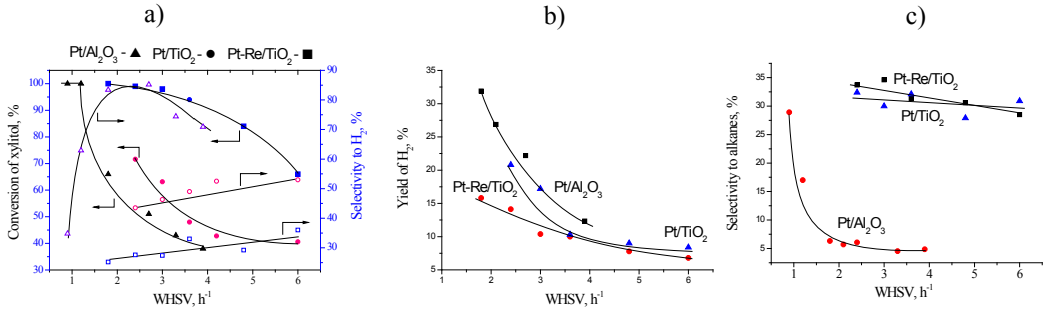

Fig. 16. Comparison of Pt/Al_2O_3 and $Pt(M)/TiO_2$ catalysts in APR of xylitol [**IV**].

the whole range of space velocities studied (Fig. 16). These results are in good correspondence with literature data on APR of glycerol over Pt supported on metal oxides[37].

The effect of the support basicity was also demonstrated in the APR of xylitol over $Pt/Mg(Al)O_x$ catalysts. Under semi-batch conditions, Pt/Mg(Al)O was proven to be more active in APR of xylitol in terms of the H_2 production compared to Pt/Al_2O_3 and it also displayed higher H_2 selectivity and suppressed alkane formation (see publication 1 from the list of related publications). This trend has been previously observed in glycerol APR[23]. The use of a basic support Mg(Al)O suppressed methane formation, a side reaction which typically causes a decrease of the H_2 selectivity. At lower feed flows, the xylitol conversion was higher in the case of Pt/Al_2O_3 than Pt/Mg(Al)O; the H_2 production was higher for the latter catalyst. The higher selectivity of Pt/Mg(Al)O was in accordance with the results obtained under semi-batch conditions.

In the aqueous-phase reforming process, formation of hydrogen and alkanes are competing with each other. Moreover, formation of alkanes requires substantial amounts of hydrogen since it proceeds through multiple deoxygenation steps. Therefore, additional acidity is required if the aim is to synthesize hydrocarbons in the aqueous phase reforming. Recent studies on bimetallic Pt-Re catalysts supported on carbons revealed elevated hydrocarbon formation during APR of glycerol compared to monometallic catalysts[40]. The study of Zhang et. al. attempted to determine the reasons for that behavior reporting an increase in Pt charge with an increase of amount of Re added[41]. In the present study, it was| demonstrated that addition of Re to Pt/TiO_2 has a significant effect on catalytic properties of the material. Essentially higher conversions of xylitol were observed in the case of bimetallic catalyst compared to the monometallic one supported on titania (Fig. 16a). Lower selectivity to hydrogen in the case of the Pt-Re sample compared to the Pt/TiO_2 catalyst imply that the addition of Re changes surface acid-basic properties of the catalytic material substantially. As anticipated, with lower selectivities and yields to hydrogen, PtRe bimetallic catalyst is slightly superior in terms of hydrocarbon formation as can be seen from Fig. 16c. It is important to note that Re itself has no remarkable catalytic activity in the APR process as revealed by many studies on glycerol APR[28,34,40]. The addition of Re changes both the number of acid sites and their strength. Zhang et al. demonstrated that the addition of Re increases the amount of acid sites in Pt/C catalysts[41]. In the present study, it was demonstrated that in the case of titania supported Pt catalysts, the addition of Re in fact leads to a decrease in the number of acid sites; however, the strength of these acid sites slightly increases. Therefore, the $Pt\text{-}Re/TiO_2$

has a better performance in terms of hydrocarbon production while monometallic catalyst is more suitable for production of hydrogen.

The dramatic effect of the catalyst acidity on hydrocarbon formation in the APR was also observed over a series of Pt supported on various carbon carriers [**V**]. The textural and acidic properties of the catalysts studied are presented in Table 1 and Table 2, respectively.

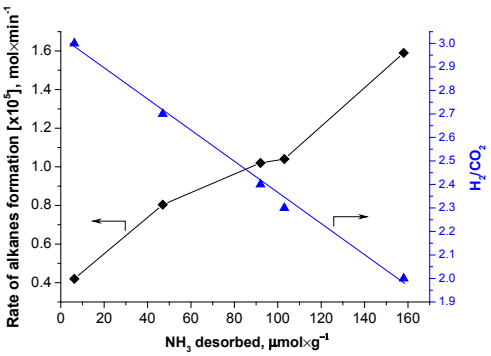

Fig. 17. Dependence of alkane formation rate and H_2/CO_2 ratio in APR of xylitol versus acidity of Pt/C determined by NH_3-TPD [**V**].

The rate of alkane formation and H_2/CO_2 ratio are influenced dramatically by the amount of acid sites on the catalyst surface as illustrated by Fig. 17. As can be seen from Fig. 16, with an increase in the total acidity of the catalytic material selectivity to H_2 decreases, while, the rate of hydrocarbon production increases with an increase in Pt/C acidity.

Textural properties of Pt/C catalysts have a significant impact on the catalytic performance of these materials in APR of xylitol. Thus, results obtained at 3.0 h^{-1} showed that the highest conversion of xylitol was achieved in the case of Pt/Sibunit (1) catalyst (32%). Pt supported on TiC-CDC was able to convert 22% of xylitol, whereas the conversion for Pt/BAC and Pt/Sibunit (1) was 22 and 15%, respectively. The Pt/C (Degussa) demonstrated the lowest value of the xylitol conversion among the Pt/C catalysts investigated – 8%. Thus, the catalysts can be placed in the following order on the basis of xylitol conversion: Pt/Sibunit (1) > Pt/TiC-CDC > Pt/BAC > > Pt/Sibunit (2) > Pt/C (Degussa).

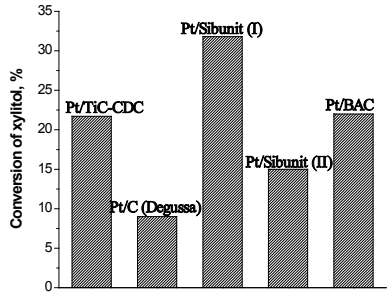

Fig 18. Conversion of xylitol over different Pt/C catalysts in the aqueous phase reforming at 3.0 h^{-1} [**V**].

Conversion of the substrate in the APR does not represent itself the transformation into target products since the initial feed can be destructed via several pathways including dehydrogenation and dehydration steps (Fig. 18). The ratio H_2/CO_2 is of high significance in the APR process displaying the potential of Pt/C catalysts to selectively produce hydrogen. Moreover, as has been mentioned above, formation of hydrogen is accompanied with production of

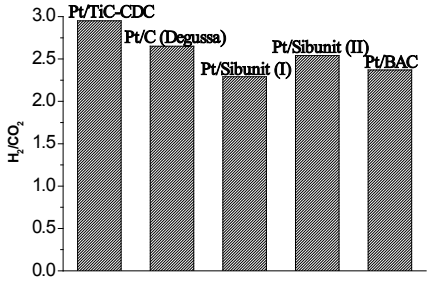

Fig 19. H_2/CO_2 ratio for different Pt/C catalysts in APR of xylitol at conversion ~ 10-12% [V].

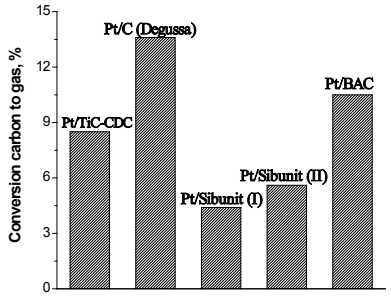

Fig 20. Conversion of carbon to gas phase for different Pt/C catalysts in APR of xylitol at conversion ~ 10-12% [V].

CO_2 in the APR process. The corresponding H_2/CO_2 ratios at xylitol conversions ca. 10-12% are shown on Fig. 19. All catalysts showed a H_2/CO_2 ratio exceeding 2.2 with Pt/TiC-CDC being the most selective (H_2/CO_2 = 2.95 at 10% conversion). Slightly less selective behavior in terms of hydrogen production was observed for Pt/C (Degussa) (2.65) and Pt/Sibunit (2) (2.53) samples. The H_2/CO_2 ratio for Pt/BAC and Pt/Sibunit (1) was 2.37 and 2.30, respectively.

The important parameter in the APR process of poyols is an ability of a catalyst to convert carbon to gaseous products, in other words, to cleave C-C bonds in the substrate. The conversion of carbon to gas in APR of xylitol is shown in Fig. 20. As can be noted, the leading catalyst is Pt/C (Degussa) with 13.6% of carbon converted to the gaseous products at 10% of xylitol conversion. The Pt/BAC catalyst was able to convert 10.5% of carbon, whereas the corresponding values found for Pt/TiC-CDC, Pt/Sibunit (2) and Pt/Sibunit (1) were 8.5%, 5.6% and 4.4%, respectively.

The following order on the basis of carbon converted to the gas phase can be presented:

Pt/C (Degussa) > Pt/BAC > Pt/TiC-CDC > Pt/Sibunit (2) > Pt/Sibunit (1)

During APR of xylitol formation of alkanes C_1-C_5 takes place as a result of dehydration and further hydrogenation reactions as has been discussed above. The hydrocarbon formation profile versus WHSV in the APR of xylitol over Pt/TiC-CDC catalyst is presented in Fig. 21. In general, all catalysts have similar composition of the hydrocarbon mixtures formed with C_1-C_3 dominance. Butane was found in minor quantities along with carbon monoxide. The formation rates for all hydrocarbons as well as carbon monoxide demonstrated a decreasing trend

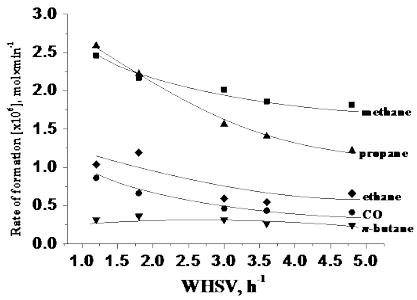

Fig 21. Composition of hydrocarbons mixture in the APR of xylitol over Pt/TiC-CDC [V].

with an increase in WHSV, or in other words, in decrease of the conversion. Pentane concentration for all experiments was below the detection limit. It might be the case that pentane was not formed, since a significantly higher surface acidity than those possessed by the used carbon-supported catalysts is required [**V**].

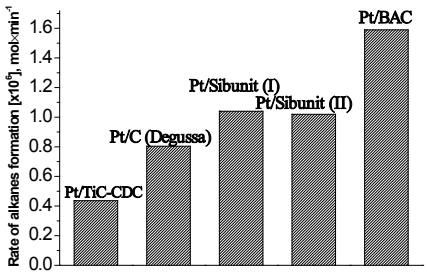

Fig 22. Rate of the hydrocarbon formation for different Pt/C catalysts in APR of xylitol. conversion ~ 10-12% [**V**].

A comparative analysis of Pt/C catalysts in terms of the hydrocarbon formation is shown in Fig. 22. The hydrocarbon formation rate in the case of Pt/BAC was more than 1.5 times higher compared to both Pt/Sibunit samples and twofold higher compared to Pt/C (Degussa). The lowest rate of the hydrocarbon formation was observed in the case of Pt/TiC-CDC which demonstrated almost a four times lower rate than Pt/BAC.

3.7 Effect of Pt cluster size on the formation of hydrogen in APR reaction [V]

Based on CO chemisorption data (Table 1), corresponding TOF values for Pt/C catalysts studied in the present research were calculated. As a result we observed a dependence of TOF_{H2} for hydrogen production on the average Pt cluster as displayed in Fig. 23. The TOF increases linearly with an increase in the average size of Pt cluster in the APR of xylitol thus indicating that APR of xylitol is a structure-sensitive reaction. Lehnert and Claus explain the increase of the hydrogen formation rate during APR of glycerol over Pt/Al_2O_3 with different dispersions, proposed that adsorption and C-C cleavage of polyol species preferably occurred on the face Pt atoms rather than on edge and corner atoms[42]. With an increase in the cluster size the number of face atoms increases whereas the number of corner and edge atoms should decline[43]. The volume of Pt clusters is proportional to r^3, while the surface area is proportional to r^2, where r – is a radius of Pt particles. Therefore, assuming that the Pt face atoms are much active in APR than edge and corner atoms, TOF should increase linearly with an increase of the average size of Pt cluster then reaching the plateu. The results regarding TOF dependence on the average size of the Pt cluster in the APR of xylitol are therefore in a very good correlation with results reported earlier for APR of glycerol and ethylene glycol.

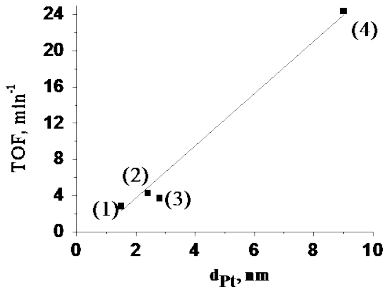

Fig 23. Dependence of TOF versus mean Pt cluster size in APR of xylitol at conversion ~10-12%. (1) – Pt/BAC, (2) – Pt/C (Degussa), (3) – Pt/Sibunit (2), (4) – Pt/TiC-CDC [**V**].

3.8 APR of xylitol over carbon- and metal oxide supported Pt catalysts: comparison

In order to study the influence of support on the catalytic activity and selectivity towards the main APR products comparison of Pt/C catlaysts and Pt/MO_x catalysts in the APR of xylitol under identical experimental conditions was performed. The data are collected in Table 3. For comparison, three carbon supported catalysts, Pt/TiC-CDC, Pt/C (Degussa) and Pt/Sibunit (2) were selected. Metal oxide supported Pt catalysts are represented by Pt/Al_2O_3 (Degussa), Pt/TiO_2 and $Pt\text{-}Re/TiO_2$. Platinum mono- and bimetallic catalysts supported on TiO_2 demonstrated the highest conversion in terms of the initial substrate conversion, conversion of carbon to gas and selectivity to alkanes compared to Pt/Al_2O_3 and Pt/C. However, the H_2/CO_2 values observed for titania supported catalysts are much lower than for other catalysts. As can be seen from Table 3, Pt/C (Degussa) demonstrated at 1.2 h^{-1} the highest conversion of carbon to gas phase products compared to other Pt/C catalysts and Pt/Al_2O_3. Carbon supported catalyst displayed a higher conversion of carbon to gas at the same level of xylitol conversion as Pt supported on Al_2O_3. A similar trend has been observed by Kim et al.[34] for APR of glycerol over Pt-Re catalysts supported on carbonaceous materials CMK-3, oxide supports as well as SiO_2 at 250°C, 45 bar and 2.0 h^{-1}. The order on the basis of carbon conversion to gas at 1.2 h^{-1} is the following one: Pt/C (Degussa) > Pt/Sibunit (2) > Pt/TiC-CDC > Pt/Al_2O_3. Shabaker et al.[44] has reported higher carbon turnover frequencies, in other words rates of carbon conversion to the gas phase, in APR of ethylene glycol: the total carbon TOF (comprises CH_4, CO_2 and C_2H_6) in the case of Pt/C was 4.88 min^{-1} whereas for Pt/Al_2O_3 it was 3.07 min^{-1}.

Table 3 Catalytic data for APR of xylitol over Pt/C at different weight hour space velocities.

	Pt/TiC-CDC			Pt/C Degussa			Pt/Sibunit I			Pt/Sibunit II			Pt/BAC			Pt/Al_2O_3			Pt/TiO_2		$Pt-Re/TiO_2$	
WHSV, h^{-1}	1.2	3.0	4.8	1.2	3.0	4.8	1.2	3.0	4.8	1.2	3.0	4.8	1.2	3.0	4.8	1.2	3.0	4.8	3.0	4.8	3.0	4.8
Conversion, %	56	12	11	57	9	3	73	32	1	57	15	13	76	22	15	82	43	27	63	43	98	84
C_{gas}, %	23.3	8.5	5.0	38.5	13.6	7.1	31.9	14.0	7.4	32.6	12.4	5.6	49.0	15.9	10.5	39.1	16.6	8.8	37.2	17.1	38.0	26.7
H_2/CO_2	2.0	2.8	3.0	2.2	2.7	2.9	1.9	2.3	2.6	1.8	2.4	2.5	1.8	2.0	2.4	2.5	2.7	2.9	1.5	1.6	0.9	0.9
S_{alk}, %	19	14	1	15	12	11	21	17	14	22	17	14	22	19	19	4.6	4.9	4.2	30	28	35	30

Conditions: 0.5 g of catalyst, 225°C, 29.3 bar, 10 wt.% xylitol solution, 30 ml×min^{-1} nitrogen flow rate

Table 4. Comparison between Pt/C catalysts and Pt/Al_2O_3 in the APR of xylitol.

Catalyst	Pt content, wt.%	D[a], %	Carbon to gas, %	H_2/CO_2	S_{alk},%	TOF_{H2}, min^{-1}	TOF_{alk}, min^{-1}
Pt/TiC-CDC	2.8	12	23.3	2.0	19	16.7	0.80
Pt/C (Degussa)	5	47	38.5	2.2	15	4.0	0.16
Pt/Sibunit(2)[b]2	5	41	32.6	1.8	22	3.0	0.24
Pt/Al_2O_3	5	30	21.1	2.5	4.6	8.5	0.10

[a]Calculated based on the information provided by CO chemisorption, [b]Pt/Sibunit (2) – corresponds to the Pt/Sibunit from H_2PtCl_6, Conditions: 0.5 g of catalyst, 225°C, 29.3 bar, 10 wt.% xylitol solution, 30 ml×min^{-1} nitrogen flow rate, conversion of xylitol ~55-57%

The H_2/CO_2 ratio for the catalysts studied decreases in the following order:

$$Pt/Al_2O_3 > Pt/C\ (Degussa) > Pt/TiC\text{-}CDC > Pt/Sibunit\ (2) > Pt/TiO_2 > Pt\text{-}Re/TiO_2$$

Likewise, Kim et al. observed the difference in selectivity to hydrogen for Pt-Re supported catalysts in APR of glycerol[34]. Pt-Re supported on alumina was the most selective catalyst, and SiO_2-supported catalyst demonstrated selectivity comparable to the CMK-3-supported material. The lowest selectivity to H_2 was observed in the case of Pt-Re/AC.

Since the production of hydrogen competes with generation of hydrocarbons in the APR process, the catalysts which demonstrated the lowest H_2/CO_2 values possessed the higher selectivity to alkanes. Thus, the selectivity to alkanes decreases in the following order:

$$Pt\text{-}Re/TiO_2 > Pt/TiO_2 > Pt/Sibunit\ (2) > Pt/TiC\text{-}CDC > Pt/C\ (Degussa) > Pt/Al_2O_3$$

The results are in a good correlation with literature on APR of glycerol[34].

Based on the data obtained from CO chemisorption, the corresponding values of turn-over frequencies of hydrogen and alkanes formation can be calculated (Table 4). As can be noted, the highest value of TOF_{H2} was observed in the case of Pt/TiC-CDC catalyst being equal to 16.7 min^{-1}. Pt/Al_2O_3 demonstrated almost twofold less value of TOF_{H2} 8.5 min^{-1} compared to Pt/TiC-CDC. The TOF of H_2 values for Pt/C (Degussa) and Pt/Sibunit (2) were 4.0 and 3.0 min^{-1}, respectively. It is worth to mention that Pt supported on carbon turned out to be more catalytically active also in hydrocarbon production via APR than Pt/Al_2O_3 as evidenced by the corresponding TOF_{alk} values presented in Table 4. Thus TOF_{alk} value in APR of xylitol decreases in the following order:

$$Pt/TiC\text{-}CDC > Pt/Sibunit\ (2) > Pt/C\ (Degussa) > Pt/Al_2O_3$$

Shabaker et al.[44] reported efficient catalytic performance of carbon supported catalysts compared to Pt/Al_2O_3 in the APR of ethylene glycol in terms of hydrogen and hydrocarbon production. The superior catalytic behavior of Pt/C catalysts, especially Pt/TiC-CDC, compared to the alumina supported sample, can be linked to higher surface areas of Pt/C materials and enhanced hydrothermal stability under severe APR conditions. Similarly to the case of CMK-3 catalysts[34], the narrow pore size distribution inside carbide-derived materials as well as regular structure and high surface area may facilitate APR, thus resulting in enhanced TOF_{H2} and TOF_{alk}.

3.9 Kinetic modeling of aqueous-phase reforming [VI]

For mathematical modeling, the kinetics data obtained for aqueous-phase reforming of sorbitol [**I**] were used. To our best knowledge, there is only one article describing kinetic modeling of glycerol APR in a batch reactor[45]. Additionally, there is an article by Moreno et. al. proposing the model based on automated network generation method described sorbitol hydrodeoxygenation (i.e. APD/H) in the presence of Pt/SiO_2-Al_2O_3[46] .

Prior to obtaining the experimental catalytic data which were further used for modeling the absence of external and internal diffusion limitations was verified in APR of sorbitol (see Section 3.2 Mass transfer effects).

Two main reaction transformation paths for a particular sugar alcohol were considered (analogously to Fig. 14). For development of the kinetic model, the main pathways of sorbitol transformation during APR were chosen on the basis of experimental data obtained earlier [**I,III**] and the current understanding of the reaction mechanism.

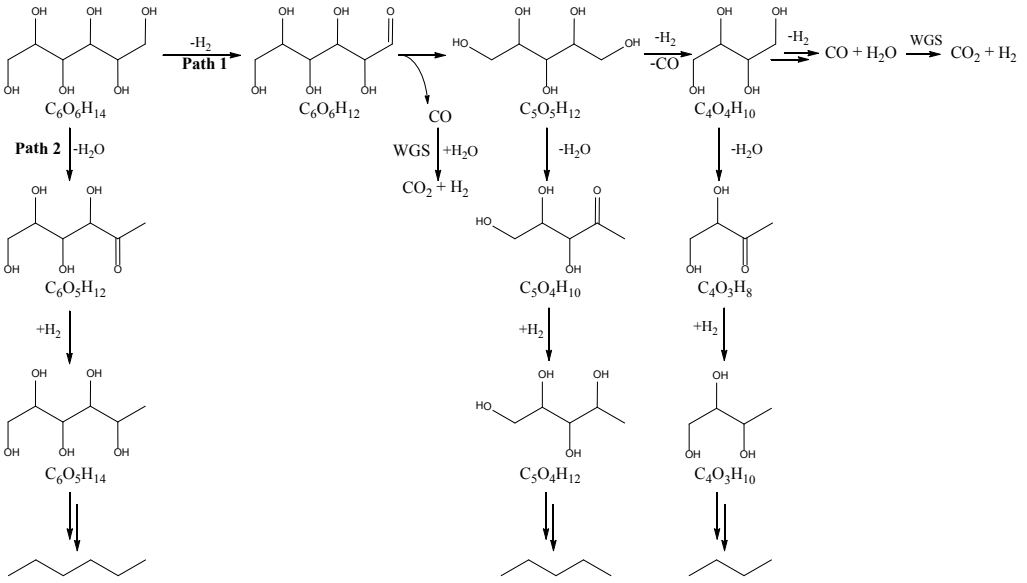

Fig. 24. The main pathways of sorbitol transformations during APR chosen for mathematical modeling of kinetics

On acidic sites, sorbitol undergoes dehydration to a ketone (Path 2 in Fig. 24) with subsequent hydrogenation to a C_6 alcohol with one hydroxyl group less than the starting sorbitol. This initial step of dehydration is considered to be the rate determining one, while the subsequent rapid steps of hydrogenation – dehydration – hydrogenation were merged together. A similar concept was applied for all alcohols of $C_nO_nH_{2n+2}$ type. Since C_6 and C_5 alkanes (i.e. hexane and pentane) as well as

methane were observed in the reaction products in inferior quantities [**I**] it is sufficient to consider the formation of C_2-C_4 alkanes only.

The path to alcohols $C_nO_nH_{2n+2}$ with n <6 (Path 1 in Fig. 24) starts with dehydrogenation on the metal sites leading to a corresponding aldehyde. These steps (for different alcohols) were assumed to be rate limiting, while decarbonylation steps were considered to be fast ones. In addition to these two main paths, water-gas shift reaction (route $N^{(5)}$) was included in the mechanism, which comprised eight reaction routes:

$N^{(1)}$: $C_6O_6H_{14} = C_5O_5H_{12} + H_2 + CO$

$N^{(2)}$: $C_5O_5H_{12} = C_4O_4H_{10} + H_2 + CO$

$N^{(3)}$: $C_4O_4H_{10} = C_3O_3H_8 + H_2 + CO$

$N^{(4)}$: $C_3O_3H_8 = C_2O_2H_6 + H_2 + CO$

$N^{(5)}$: $CO + H_2O = CO_2 + H_2$,

$N^{(6)}$: $C_4O_4H_{10} + 4H_2 = C_4H_{10} + 4H_2O$

$N^{(7)}$: $C_3O_3H_8 + 3H_2 = C_3H_8 + 3H_2O$,

$N^{(8)}$: $C_2O_2H_6 + 2H_2 = C_2H_6 + 2H_2O$

The rates for reaction on metal sites

$$r^{(1)} = k_2\theta_{C_6O_6H_{14}} = k_2K_1C_{C_6O_6H_{14}}\theta_V = \\ = \frac{k_2K_1C_{C_6O_6H_{14}}}{1 + K_1C_{C_6O_6H_{14}} + K_3C_{C_5O_5H_{12}} + K_5C_{C_4O_4H_{10}} + K_7C_{C_3O_3H_8} + K_9C_{C_2O_2H_6} + K_{10}C_{H_2O}} \quad (8)$$

The rates along the second, third and fourth routes are given in a similar fashion

$$r^{(2)} = \frac{k_4K_3C_{C_5O_5H_{12}}}{1 + K_1C_{C_6O_6H_{14}} + K_3C_{C_5O_5H_{12}} + K_5C_{C_4O_4H_{10}} + K_7C_{C_3O_3H_8} + K_9C_{C_2O_2H_6} + K_{10}C_{H_2O}} \quad (9)$$

$$r^{(3)} = \frac{k_6K_5C_{C_4O_4H_{10}}}{1 + K_1C_{C_6O_6H_{14}} + K_3C_{C_5O_5H_{12}} + K_5C_{C_4O_4H_{10}} + K_7C_{C_3O_3H_8} + K_9C_{C_2O_2H_6} + K_{10}C_{H_2O}} \quad (10)$$

$$r^{(4)} = \frac{k_8 K_7 C_{C_3O_3H_8}}{1 + K_1 C_{C_6O_6H_{14}} + K_3 C_{C_5O_5H_{12}} + K_5 C_{C_4O_4H_{10}} + K_7 C_{C_3O_3H_8} + K_9 C_{C_2O_2H_6} + K_{10} C_{H_2O}} \quad (11)$$

The rate along the route $N^{(5)}$ can be defined through either of the steps 10 and 11, thus

$$r^{(5)} = \frac{k_{11} C_{H_2O} C_{CO}}{1 + K_1 C_{C_6O_6H_{14}} + K_3 C_{C_5O_5H_{12}} + K_5 C_{C_4O_4H_{10}} + K_7 C_{C_3O_3H_8} + K_9 C_{C_2O_2H_6} + K_{10} C_{H_2O}} \quad (12)$$

Similarly for the reactions routes occurring on the support sites the reaction rates could be formulated

$$r^{(6)} = \frac{k_{13} K_{12} C_{C_4O_4H_{10}}}{1 + K_{12} C_{C_4O_4H_{10}} + K_{14} C_{C_3O_3H_8} + K_{16} C_{C_2O_2H_6}} \quad (13)$$

$$r^{(7)} = \frac{k_{15} K_{14} C_{C_3O_3H_8}}{1 + K_{12} C_{C_4O_4H_{10}} + K_{14} C_{C_3O_3H_8} + K_{16} C_{C_2O_2H_6}} \quad (14)$$

$$r^{(8)} = \frac{k_{17} K_{16} C_{C_2O_2H_6}}{1 + K_{12} C_{C_4O_4H_{10}} + K_{14} C_{C_3O_3H_8} + K_{16} C_{C_2O_2H_6}} \quad (15)$$

Finally, the generation rates of compounds can be written as;

$$-\frac{dC_{C_6O_6H_{14}}}{d\tau} = r^{(1)}, \frac{dC_{C_5O_5H_{12}}}{d\tau} = r^{(1)} - r^{(2)}; \frac{dC_{C_4O_4H_{10}}}{d\tau} = r^{(2)} - r^{(3)} - r^{(6)}; \frac{dC_{C_3O_3H_8}}{d\tau} = r^{(3)} - r^{(4)} - r^{(7)};$$

$$\frac{dC_{C_2O_2H_6}}{d\tau} = r^{(4)} - r^{(8)}; \frac{dC_{CO}}{d\tau} = r^{(1)} + r^{(2)} + r^{(3)} + r^{(4)} - r^{(5)}; \frac{dC_{C_4H_{10}}}{d\tau} = r^{(6)}; \frac{dC_{C_3H_8}}{d\tau} = r^{(7)};$$

$$\frac{dC_{C_2H_6}}{d\tau} = r^{(8)}; \frac{dC_{H_2}}{d\tau} = r^{(1)} + r^{(2)} + r^{(3)} + r^{(4)} + r^{(5)} - 4r^{(6)} - 3r^{(7)} - 2r^{(8)}; \quad (16)$$

where τ is the residence time.

The kinetic modeling comprised all the reaction rates listed above. For the estimation of parameters, a set of differential equations describing the changes in the concentrations profiles of the reagents and products along the reactor length was solved by means of ModEst software[47].

In fact, the model, based on Eqs. (8)-(16), was overparameterized. The presence of adsorption coefficients in the denominators resulted in too large errors during parameters estimation. Hence, a simplified version of the model was developed. For that purpose K_1, K_3. K_5, K_{12}, K_{14} and K_{16} were approximated to zero in the model. Moreover, further simplifications were possible, since CO was not observed in the gas phase, thus the oxygen on the surface can be neglected. Therefore, the modified model which comprised equations (17)-(24) was obtained:

$$r^{(1)} = k_2^{'} C_{C_6O_6H_{14}} \tag{17}$$

$$r^{(2)} = k_4^{'} C_{C_5O_5H_{12}} \tag{18}$$

$$r^{(3)} = k_6^{'} C_{C_4O_4H_{10}} \tag{19}$$

$$r^{(4)} = k'_8 \, C_{C_3O_3H_8} \tag{20}$$

$$r^{(5)} = k_{10} C_{H_2O} \tag{21}$$

$$r^{(6)} = k'_{13} \, C_{C_4O_4H_{10}} \tag{22}$$

$$r^{(7)} = k'_{15} \, C_{C_3O_3H_8} \tag{23}$$

$$r^{(8)} = k'_{17} \, C_{C_2O_2H_6} \tag{24}$$

These modified constants contain also the adsorption coefficients.

Additionally in order to satisfy the mass balance one more reaction was added to the model accounting for formation of other components from the reactant, for example furans:

$$r^{(9)} = k'_{18} \, C_{C_3O_3H_8} \tag{25}$$

This simplified model did not affect the generation rates written in Eq. (16) except for the substrate consumption rate, which is converted to

$$-\frac{dC_{C_6O_6H_{14}}}{dt} = r^{(1)} + r^{(9)} \tag{26}$$

Using Levenberg-Marquardt simplex method, the target function, which was defined as the incompliance between the experimental and calculated values of concentrations was used to minimize the objective function. The sum of the residual squares was minimized using the following objective function

$$Q = \left\| C_{\exp} - C_{est} \right\|^2 = \sum_t \sum_i \left(C_{\exp,it} - C_{est,it} \right)^2 \quad (27)$$

Where C_{exp} is the experimental value and C_{est} denotes the predictions given by the model, i is the component index and t is the time value. The quality of the fit and accuracy of the model description was defined by the degree of explanation R^2; which reflects comparison between the residuals given by the model to the residuals of the simpliest model one may think of, i.e. the average value of all the data points.

The R^2 value is given by the expression

$$R^2 = 100 \frac{(y_{model} - y_{experiment})^2}{(y_{model} - \bar{y}_{experiment})^2} \quad (28)$$

The overall residual sum of squares for all the products was 0.1595×10^{-6}.

The values of the calculated frequency factors, and as well as the estimated relative standard errors (in %) of the tested reaction mechanism based on Eqs. (16)-(26) are presented in [**VI**].

Fig. 25 displays a comparison between the experimental obtained data and model predictions for CO_2 and hydrogen formation in the APR of sorbitol at different conditions (WHSV). Conversion of sorbitol was 100% for all experimental points.

As can be seen from Fig. 25a, hydrogen formation increases with an increase in WHSV in agreement with experiments. In accordance with the results reported earlier, more hydrogen was observed at higher space velocities, in other words, at lower contact times. The results are understandable since at higher contact times hydrogen is more consumed in various hydrogenation reactions.

Formation of CO_2 predicted by the model as a function of WHSV is shown on Fig. 25b. The results are in a good correlation with the experimental data obtained and confirm the ability of the model to describe at least the main trends in the formation of hydrogen and CO_2 as a function of WHSV.

Fig. 26 displays a comparison between predicted corresponding carbon flows for C_3 and C_6 compounds present in the liquid phase during APR of sorbitol and the experimental data. As can be seen from Figure 26 the model is able to predict rather well the carbon flows for major liquid products, C_3 and C_6 (with the degree of explanation above 97%) which are present in the liquid phase in higher concentration compared to other products. Liquid products containing two, four and

five carbon atoms in the structures were also included in the model; however, the error of description was rather large.

It should be noted that deviations from the experimental data were also observed for calculated values of hydrocarbons. Compounds C_xH_y were included in the model, but due to significantly lower concentration of each hydrocarbon component compared to CO_2 and hydrogen the error was large.

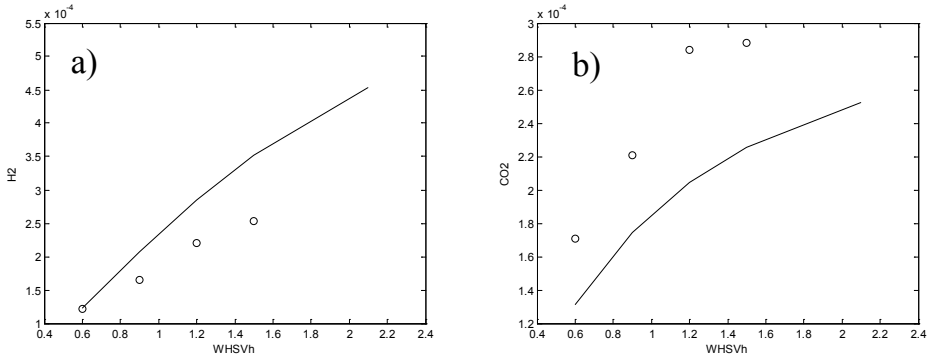

Fig. 25. Fit of the model to the experimental data: a) formation of hydrogen and b) carbon dioxide as a function of WHSV in the APR of sorbitol. Conditions: 1 g of catalyst, 498 K, 29.3 bar, N_2 flow 30 ml×min^{-1}, 10 wt.% sorbitol solution, conversion 100%.

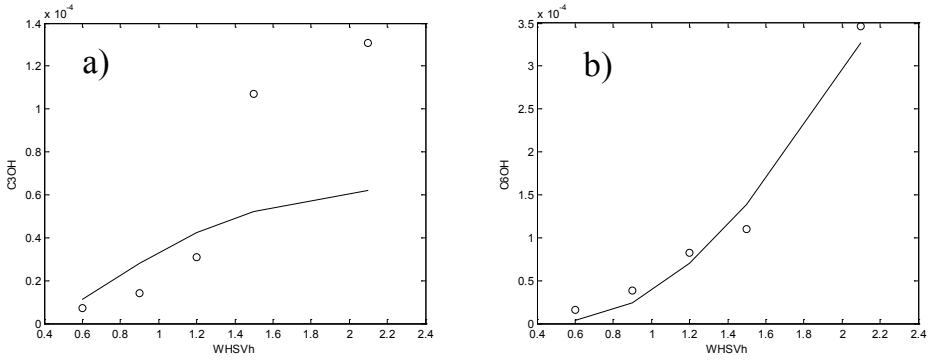

Fig. 26. Fit of the model to the experimental data: a) formation of C_3 (carbon flow) and b) C_6 products (carbon flow) in the liquid phase a function of WHSV in the APR of sorbitol. Conditions: 1 g of catalyst, 498 K, 29.3 bar, N_2 flow 30 ml×min^{-1}, 10 wt.% sorbitol solution, conversion 100%.

4. Conclusions

Aqueous phase reforming of the two most abundant sugar alcohols stemming from biomass, sorbitol and xylitol, was studied in a continuous fixed-bed reactor over supported Pt and Pt-Re catalysts. The catalysts demonstrated a stable performance within 160 h time-on-stream.

Optimization of reaction parameters aiming at selective production of hydrogen was performed. For Pt/Al_2O_3, the high catalytic activity for hydrogen production from sugar alcohols was observed with up to 85% of selectivity to hydrogen.

Based on the analysis of the principal APR products, H_2 and CO_2, as well as on the analysis of the liquid-phase products, a more complete understanding about the reaction network for polyols APR was achieved and an advanced reaction network describing the formation of the main products and intermediates was proposed.

The structure of the substrate has a substantial impact on the hydrogen yield and selectivity in APR. Thus, higher yields of hydrogen were observed in the case of a substrate possessing a shorter carbon chain (xylitol) compared to longer chain substrates (sorbitol).

The effect of the support (TiO_2, C), as well as addition of the second metallic component (Re), on aqueous phase reforming of polyols was studied. It was shown that acid-basic properties of the support play a significant role in directing the reaction towards the formation of hydrogen or hydrocarbons. Addition of the Re to Pt increases acidic properties of the catalytic material, thus enhancing the formation of alkanes compared to monometallic catalysts.

For the first time, a structure sensitivity of higher polyols (xylitol) was demonstrated using a series of Pt/C catalysts. It was found that turn-over frequency linearly increases with an increase in the average Pt cluster size.

The reaction kinetics was modeled based on mechanistic considerations for sorbitol transformation during APR. The kinetic model was compared with experimental data through numerical data fitting showing a reasonably good correspondence (with degree of explanation for C_6 products above 97%). Further improvements in the model are desirable to incorporate the formation of gas and liquid-phase products over a broader conversion range.

In conclusion, APR is an attractive method for hydrogen and alkane production from renewables. By altering the process parameters, a choice of catalyst and the feed, the reaction can be steered to the formation of hydrogen or alkanes.

5. References

[1] Thermochemical Conversion of Biomass to Liquid Fuels and Chemicals, editor Mark Crocker, RSCPublishing, 2010.
[2] S. Ivanova, C. Petit, V. Pitchon, *Appl. Catal. A*, 2004, 267, 191-201.
[3] A. Tanksale, Y. Wong , J.N. Beltramini, G.Q. Lu, *Int. J. Hydr. En*., **2007**, *32*, 717–724.
[4] A. Aho, N. Kumar.,K Eränen K., P. Backman, M. Hupa, T. Salmi, D.Yu Murzin., *Catal. in Industry*, **2008**, *2*, 49–51.
[5] D. Simonetti, J.A. Dumesic, *Catal. Rev.*, **2009**, *51*, 441-484.
[6] G.W. Huber,S. Iborra, A. Corma, *Chem. Rev.*, **2006**, *106*, 4044–4098.
[7] C.-H. Zhou, X, Xia, Ch.-X. Lin, D.S. Tonga and J. Beltramini, *Chem. Soc. Rev.*, **2011**, *40*, 5588–5617.
[8] J.C. Serrano-Ruiz, R. Luque, A. Sepulveda-Escribano, *Chem. Soc. Rev.,* **2011**, *40*, 5266–5281.
[9] E. Sjöström, "Wood Chemistry – Fundamental and Applications", Academic, London, 1993.
[10] D. Fengel, G. Wegener, A. Heizmann, M. Przyklenk, *Cell. Chem. Tech.*, **1978**, *12*, 31-37.
[11] S. Willför, A. Sundberg, A. Pranovich, B. Holmbom, *Wood. Sci. Technol.*, **2005**, *39*, 601-617.
[12] http://www.starch.dk/
[13] R.D. Cortright, R.R. Davda, J. A. Dumesic, *Nature*, **2002**, *418*, 964-967.
[14] R.R. Davda and J.A. Dumesic, *Angew. Chem. Int. Ed*., **2003**, *42*, 4068 –4071.
[15] G.W. Huber, J. Chheda, C. B. Barrett and J.A. Dumesic, *Science*, **2005**, *308*, 1446-2079.
[16] R.R. Davda, J.W. Shabaker, G.W. Huber, R.D. Cortright, J.A. Dumesic, *Appl. Catal. B: Environ.*, **2005**, *56*, 171-186.
[17] N. Li, H. Huber, *J. Catal.*, **2010**, *270*, 48–59.
[18] Y.T. Kim, J.A. Dumesic, G.W. Huber, *J. Catal.*, **2013**, *304*, 72–85.
[19] K. Murata, Isao T., M. Inaba, *React. Kinet. Catal. Lett.*, **2008**, *93*, 59-66.
[20] D.A. Simonenti, E.L. Kunkes, J.A. Dumesic, *J. Catal.*, **2007**, *247*, 298-306.
[21] Virent System Inc."Hydrogen Generation from Biomass-Derived Carbohydrates via the Aqueous-Phase Reforming (APR) Process", DOE Hydrogen Program, FY 2007 Annual Progress Report.
[22] "Exceptional Jet Fuel Produced From High-Quality Cellulosic Sugars", Virent Systems Inc. Newsletter, March 26, 2012.
[23] D.A. Boga, R.Oord, A.M. Beale, Y.-M. Chung, P.C.A. Bruijnincx, B.M. Weckhuysen, *ChemCatChem*, **2013**, *5*, 529–537
[24] J. Sa , C. Kartusch, M. Makosch, C. Paun, J. A. van Bokhoven, E. Kleymenov, J. Szlachetko, M. Nachtegaal, H. G. Manyar, C. Hardacre, *Chem. Commun.*, **2011**, ***47***, 6590–6592.
[25] G.J. den Otter, D.T. Dautzenberg, *J. Catal.*, **1978**, *53*, 116-125.
[26] R. Burch, C. Paun, X.-M. Cao, P. Crawford, P. Goodrich, C. Hardacre, P. Hu, L. McLaughlin, J. Sá, J.M. Thompson, *J. Catal.*, **2001**, *283*, 89-97.
[27] K.G. Azzam, I.V. Babich, K. Seshan, L. Lefferts, *J. Catal.*, **2007**, *251*, 163-171.
[28] L. Zhang, A.M. Karim, M.H. Engelhard, Z. Wei, D.L. King,, Y. Wang, *J. Catal.*, **2012**, *287*, 37–43.
[29] P. Serp, J.L. Figueiredo, "Carbon Materials for Catalysis", Philippe Serp, José Luis Figueiredo, John Wiley & Sons 2009.
[30] D. Murzin, "Enginering Catalysis", Walter De Gruyter, Berlin/Boston, 2013.
[31] R. M. Ravenelle, J. R. Copeland, W.-G. Kim, J.C. Crittenden, C Sieverse, *ACS Catalysis*, **2010**, *1*, 552-561
[32] R.M. Ravenelle, J.R. Copeland, A.H. Van Pelt, J.C. Crittenden, C. Sievers, *Top. Catal.*, **2012**, *55*, 162–174.
[33] L. Giordano, R. Calabrese, E. Davoli, D. Rotilio, J. Chromat, **2003**, *1017*, 141-149.

[34]H.-D. Kim, H.J. Park, T.-W. Kim, K.-E. Jeong, H.-J. Chae, S.-Y. Jeong, C.-H. Lee, C.-U. Kim, *Catal. Today*, **2012**, *185*, 73-80.
[35] A. Wawrzetz, B. Peng, A. Hrabar, A. Jentys, A.A. Lemonidou, J.A. Lercher, *J. Catal.*, **2010**, *269*, 411-420.
[36] A.O. Menezes, M. T. Rodrigues, A. Zimmaro, L.E.P. Borges, M.A. Fraga, *Renew. Energy*, **2011**, *36*, 595-599.
[37] Y. Guo, M. U. Azmat, X. Liu, Y. Wang, G. Lu, *Appl. Energy*, **2012**, *92*, 218–223.
[38] V. Dal Santo, A. Gallo, A. Naldoni, M. Guidotti, R. Psaro, *Catal. Today*, **2012**, *197*, 190– 205
[39] "Catalysis by metal alloys", Studies in Surface Science and Catalysis, Volume 95, 1995.
[40] a) R.R. Soares, D.A. Simonetti, J.A. Dumesic, *Angew. Chem. Int. Ed*., **2006**, *45*, 3982-3985, b) D.A. Simonenti, E.L. Kunkes, J.A. Dumesic, *J. Catal.*, **2007**, *247*, 298-306, c) E.L. Kunkes, D.A. Simonetti, J.A. Dumesic, W.D. Pyrz, L.E. Murillo, J.G. Chen, D.J. Buttrey, *J. Catal.*, **2008**, *260*, 164-177, d) E.D. Kunkes, R.R. Soares, D.A. Simonetti, J.A. Dumesic, *App. Catal. B. Environ.*, **2009**, *90*, 693-698, e) D.L. King, L. Zhang, G. Xia, A.M. Karim, D.J. Heldebrant, X. Wang, T. Peterson, Y. Wang, *Appl. Catal. B. Environ.*,, **2010**, *99*, 206-213.
[41] L. Zhang, A. Karim, M. Engelhard, Z. Wei, D.L. King, Y. Wang, *J. Catal.*, **2012**, *287*, 37-43.
[42] K. Lehnert, P. Claus, *Catal. Comm.*, **2008**, *9*, 2543–2546.
[43] R. Van Hardeveld, F. Hartog, *Surf. Sci.*, **1969**, *15*, 189-230.
[44] J.W. Shabaker, G.W. Huber, R.R. Davda, R.D. Cortright, and J.A. Dumesic, *Catal. Lett.* **2003**, *88*, 1-8.
[45] F.Aiouache, L. McAleer, Q. Gan A.H. Al-Muhtaseb, M.N. Ahmad, *Appl. Catal. A. Gen.,* **2013**, *466*, 240-255.
[46] B.M. Moreno, N. Li, J. Lee, G.W. Huber, M.T. Klein, *RSC Adv.*, **2013**, doi: 10.1039/c3ra45179h.
[47] Haario, H. ModEst 6.0, Helsinki, 2010.

Åbo Akademi University

ISBN 978-952-12-2974-9
Painosalama Oy – Turku, Finland 2013